Ore Geology Reviews 38 (2010) 334–366

Contents lists available at ScienceDirect

Ore Geology Reviews

journal homepage: www.elsevier.com/locate/oregeorev

A continent-wide study of Australia's uranium potential Part I: GIS-assisted manual prospectivity analysis

O.P. Kreuzer [a,*], V. Markwitz [b], A.K. Porwal [a,b], T.C. McCuaig [b]

[a] Centre for Exploration Targeting, Curtin University of Technology, Kent Street, Bentley, WA 6102, Australia
[b] Centre for Exploration Targeting, University of Western Australia, 35 Stirling Highway, Crawley, WA 6009, Australia

ARTICLE INFO

Article history:
Received 3 July 2009
Received in revised form 12 June 2010
Accepted 4 August 2010
Available online 20 August 2010

Keywords:
Area selection
Conceptual targeting
Deposit classification scheme
Mineral systems approach
Prospectivity analysis
Uranium
Australia

ABSTRACT

This paper describes the approach to, and outcomes of, a manual analysis (i.e., a cognitive assessment of spatial and non-spatial data) of the uranium potential of 90 geological regions in Australia. For this analysis, the 14 principal uranium deposit types recognized by the International Atomic Energy Agency were grouped in six uranium systems models (i.e., surficial, sedimentary, igneous-related, metamorphic/metasomatic, unconformity-related, and vein-related uranium systems) on the basis of similar genetic processes, environments of ore formation and ingredients mappable at the regional to continent scale. The newly proposed uranium systems models are structured according to the mineral systems approach and focus on the critical mineralization processes that must occur for a uranium deposit to form in a particular region. Our manual prospectivity analysis employed this approach to assess the probability of the critical genetic processes having occurred in each geological region. In this semi-quantitative, probabilistic evaluation, technical, quality and opportunity ranking schemes were used to rank each geological region based on the probability of occurrence of and potential for high-quality uranium deposits and opportunity for securing prospective ground. Based on this assessment, the geological regions with the greatest potential for discovery of potentially recoverable uranium resources are the Ashburton, Broken Hill, Litchfield, McArthur, Money Shoal, Murphy, Paterson, Pine Creek and Northeast Tasmania regions (i.e., quality ranking of 10.0), the Gawler and Polda regions (i.e., 9.0), and the Amadeus, Georgetown, Stuart, Tanami regions (i.e., 8.1). Most of these regions contain known unconformity-related or sandstone-hosted uranium deposits, although some of them are pure conceptual plays that have received relatively little attention in terms of uranium exploration. Maps based on the numerical output of the prospectivity analysis helped to inform area selection decisions and detailed follow-up studies, and focus time and resources. The template developed in this study can easily be modified to suit prospectivity analyses for other metals or a similar investigation in another country. As illustrated in Part II, the best possible approach to a complex, continent-wide prospectivity analysis is to harness the strengths of both manual and automated (i.e., sophisticated computational techniques applied to spatial data) approaches as these methodologies essentially address each other's limitations.

© 2010 Elsevier B.V. All rights reserved.

1. Introduction

Area selection is the critical first step in a sequence of mineral exploration activities (Lord et al., 2001) that occasionally leads to the discovery of an economic mineral deposit (Hronsky, 2004). According to Hronsky (2004) and Hronsky and Groves (2008), this selection is essentially a prediction of the probability of occurrence of a mineral deposit based on the application of geological concepts to pre-existing datasets. The inherent risk associated with this decision is one of the greatest in exploration, given the very high opportunity cost linked to exploration being conducted in a place where the targeted deposit type does not exist (Hronsky, 2004; Penney et al., 2004).

Prospectivity analysis (i.e., the spatial prediction of mineral potential), be it GIS-assisted manual (i.e., cognitive assessment of spatial and non-spatial data) or GIS-driven automated (i.e., sophisticated computational techniques applied to spatial data), can greatly reduce the technical and financial risks associated with area selection. Based on this premise, an industry sponsor engaged the Centre for Exploration Targeting, a joint venture between the University of Western Australia and Curtin University of Technology, to undertake a comprehensive assessment of the uranium potential of Australia, a continent that contains approximately 1,350,000 t U_3O_8 or 24% of the world's known recoverable uranium resources (Lambert et al. 2005; www.world-nuclear.org).

This paper reports the approach taken and results of a conceptual, manual approach to uranium prospectivity analysis. The principal

* Corresponding author. Tel.: +61 488 655 588.
E-mail address: oliverk@mitchellrivergroup.com (O.P. Kreuzer).

0169-1368/$ – see front matter © 2010 Elsevier B.V. All rights reserved.
doi:10.1016/j.oregeorev.2010.08.003

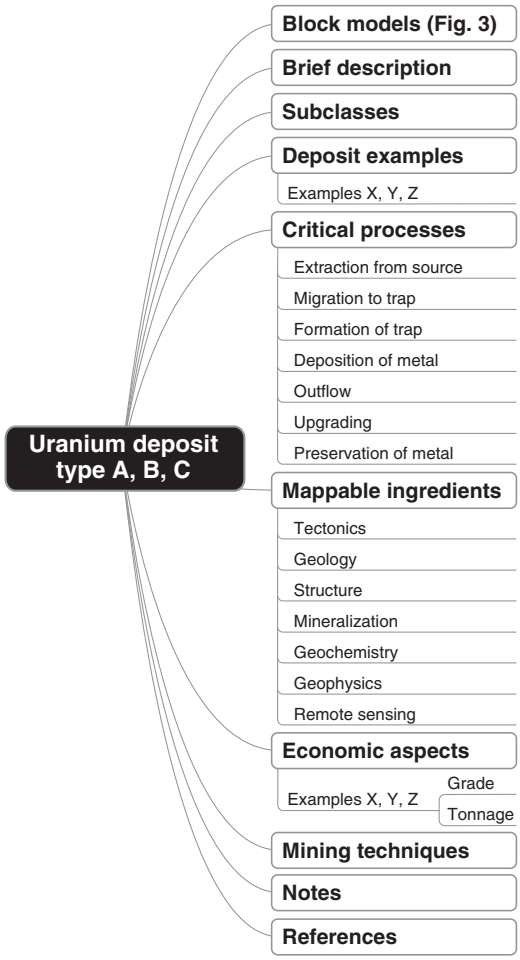

Fig. 1. Schematic representation of the standardized mind map and its main branches and sub-branches that were used for collating, organizing and clasifying the vast amount of information collected in this sudy for each of the 14 principal uranium deposit types recognized by the International Atomic Energy Agency (2000) (cf. Fig. 2a).

objectives of this study were to: (1) develop an understanding of the controls on, and genetic aspects of, uranium mineralization; (2) translate the understanding of uranium systems to exploration systems (cf. McCuaig et al., 2010); (3) identify where on the Australian continent significant uranium systems could form, and target ground based on this understanding; (4) generate exploration targets at the regional to camp-scale that satisfy designated targeting criteria; and (5) rank these targets according to the designated ranking criteria. The main academic challenge was to come up with an effective framework for this analysis. Major additional challenges included the sheer magnitude of the task, short time frame for completion, and highly competitive environment in terms of securing uranium prospective ground in Australia in the years 2006 and 2007.

The manual analysis described in this paper informed and served as a basis for a subsequent automated approach using sophisticated computational techniques and covering the same area. The results of this computer-driven analysis and the advantages of a two-pronged manual/automated approach to continent-wide prospectivity mapping are reported in a companion paper that will be submitted in early 2011.

2. Manual uranium prospectivity analysis

The key sequential steps in the manual prospectivity analysis were: (1) develop an understanding of the processes that form uranium deposits and their expressions in geoscience datasets by way of a comprehensive literature review; (2) adopt a mineral systems approach (Wyborn et al., 1994; Knox-Robinson and Wyborn, 1997) to generalize and translate existing uranium deposit models into process-based uranium system models that are suitable for a continent-wide analysis; (3) compile available geological, geochemical and geophysical data into a GIS; (4) carry out the analysis, synthesize key geological evidence in a standardized prospectivity matrix, and produce uranium prospectivity maps; and (5) identify and further evaluate ground prospective for uranium deposits.

2.1. Literature review

The first step in this study was a comprehensive review of the literature on uranium deposits with a particular focus on uranium mineralizing processes and their mappable expressions in geological, geochemical and geophysical datasets. The vast amount of information extracted from the literature was compiled into standardized hierarchical tree diagrams (i.e., mind maps) (Fig. 1) for each uranium deposit type in the authoritative classification scheme of the International Atomic Energy Agency (2000) (Fig. 2a). These mind maps served as a basis for constructing process-based uranium systems models that are more suitable for the purpose of a continent-wide prospectivity analysis.

2.2. Rationale and construction of uranium systems models

The established uranium deposit classification schemes (Dahlkamp, 1978; Mashkovtsev et al., 1995; International Atomic Energy Agency, 2000; McKay and Miezitis, 2001; OECD Nuclear Energy Agency and International Atomic Energy Agency, 2005) are invaluable for communication of scientific concepts, reference and learning. However, these schemes are largely based on and aimed towards deposit-scale studies and comprise a large number of uranium deposit types and sub-types (Fig. 2a) that translate into a large number of geological variables. Moreover, many of these geological variables are only evident at the deposit scale, whereas, at the regional to continental scale, many types of uranium deposits illustrate fundamental similarities in terms of source, transport and depositional processes (Cuney, 2009; Skirrow et al., 2009a) (Tables 1a–1e).

Creation of the uranium systems models, the conceptual foundation of this prospectivity analysis, closely followed and incorporated principles of the well-established mineral systems approach (Wyborn et al., 1994; Knox-Robinson and Wyborn, 1997). According to the mineral systems approach, the genesis of a mineral deposit requires: (1) fluid/melt, metal and ligand sources, and a source of energy that drives the mineralizing system; (2) pathways along which fluids/melts can migrate; (3) trap zones (i.e., narrow, effective pathways) along which fluid/melt flow becomes focused, fluid/melt composition is modified, and the metals of interest accumulate; and (4) outflow zones for discharge of residual fluids, or melts. As such, this approach is well-suited for prospectivity analyses (Wyborn et al., 1994; Knox-Robinson and Wyborn, 1997; Hronsky, 2004; Hronsky and Groves, 2008) because (1) in this concept the formation of a mineral deposit is precluded where a particular system lacks one or more of the essential components; (2) this concept is neither restricted to a particular geological setting nor limited to a specific mineral deposit type (rather, it allows for multiple deposit types, or sub-types, to be realized and tested within a single mineral system); (3) it requires identification of the critical genetic processes in the formation of a mineral deposit and their mappable criteria at all scales of the system (given that a mineral deposit is considered the focal point of a much larger system of energy and mass flux that control deposit size and location); (4) it promotes a multi-scale, multidisciplinary approach

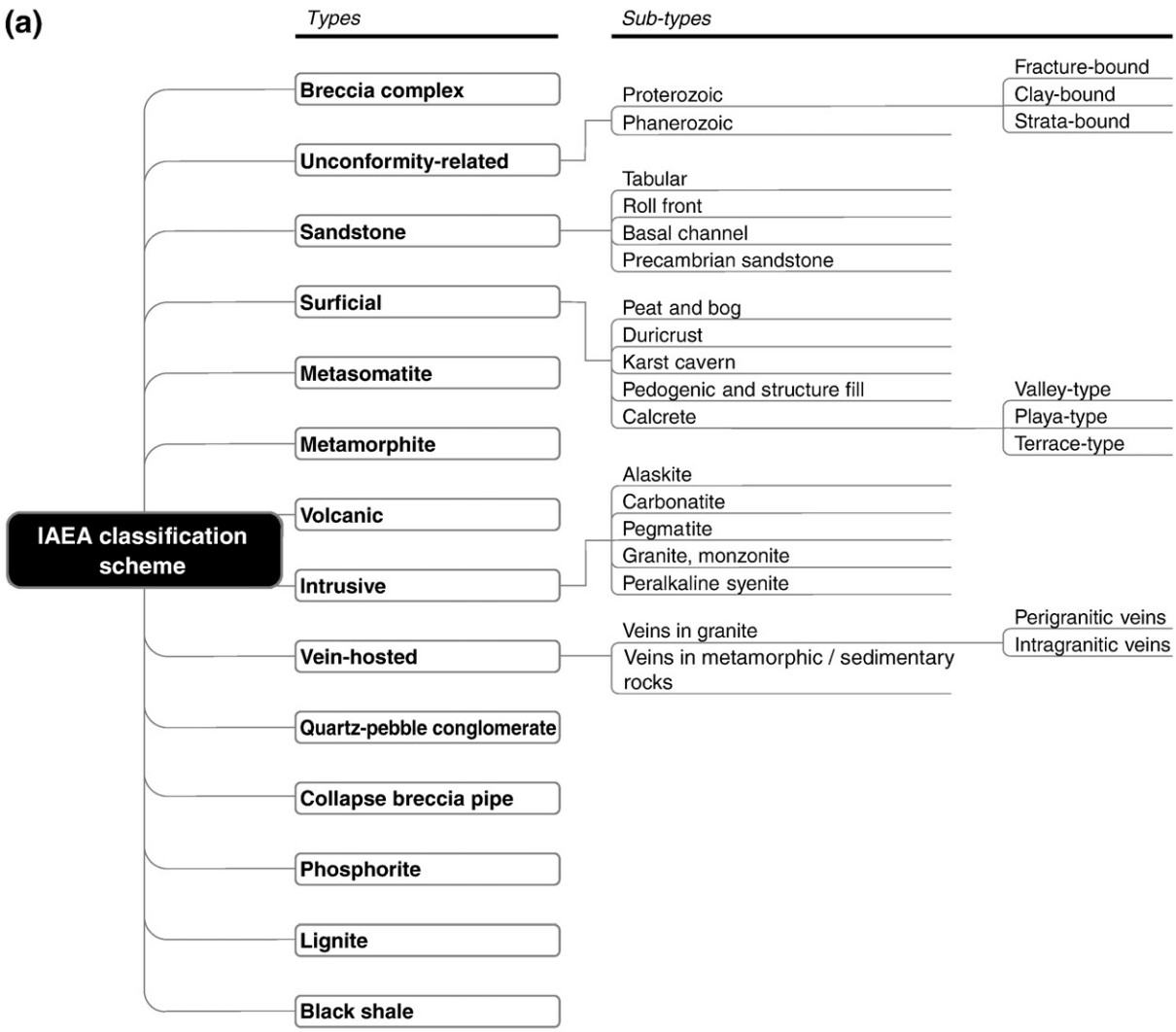
(a)
Types
Sub-types
IAEA classification scheme
Breccia complex
Unconformity-related
Sandstone
Surficial
Metasomatite
Metamorphite
Volcanic
Intrusive
Vein-hosted
Quartz-pebble conglomerate
Collapse breccia pipe
Phosphorite
Lignite
Black shale
Proterozoic
Phanerozoic
Fracture-bound
Clay-bound
Strata-bound
Tabular
Roll front
Basal channel
Precambrian sandstone
Peat and bog
Duricrust
Karst cavern
Pedogenic and structure fill
Calcrete
Valley-type
Playa-type
Terrace-type
Alaskite
Carbonatite
Pegmatite
Granite, monzonite
Peralkaline syenite
Veins in granite
Veins in metamorphic / sedimentary rocks
Perigranitic veins
Intragranitic veins

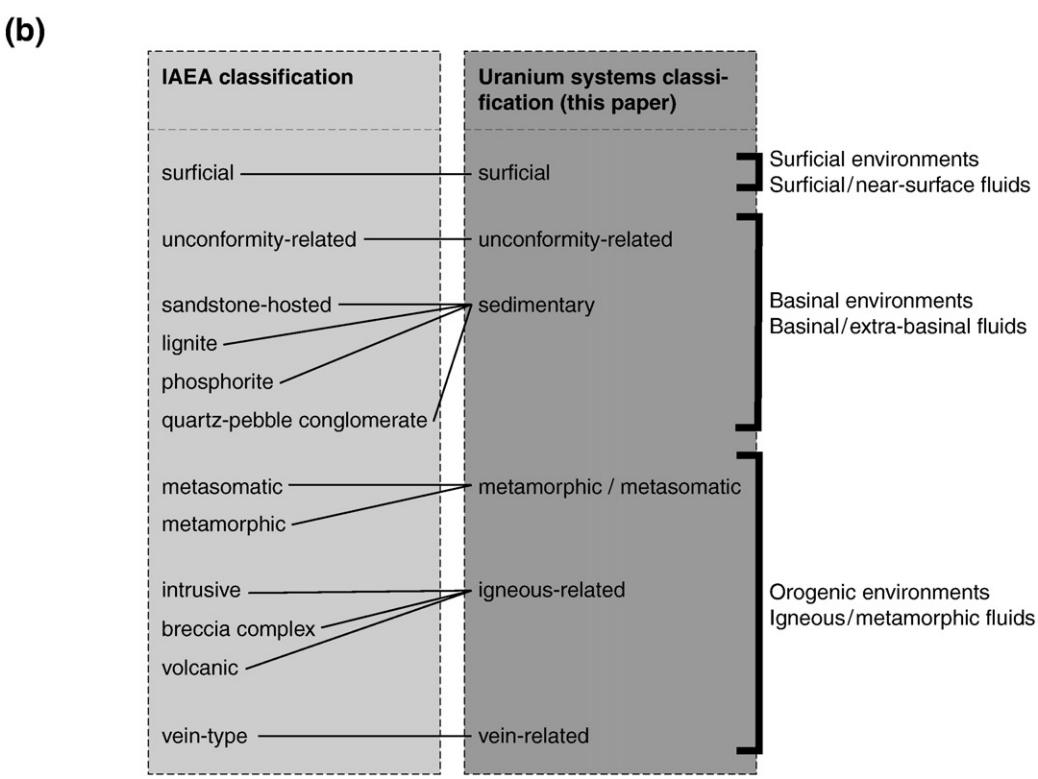
(b)
IAEA classification
Uranium systems classification (this paper)
surficial
unconformity-related
sandstone-hosted
lignite
phosphorite
quartz-pebble conglomerate
metasomatic
metamorphic
intrusive
breccia complex
volcanic
vein-type
surficial
unconformity-related
sedimentary
metamorphic / metasomatic
igneous-related
vein-related
Surficial environments
Surficial/near-surface fluids
Basinal environments
Basinal/extra-basinal fluids
Orogenic environments
Igneous/metamorphic fluids

Table 1a
Brief summary of the principal uranium deposit types and critical genetic processes and their mappable ingredients.

Uranium deposit type	Unconformity-related[1]	Breccia complex[2]
Significant examples	Cigar Lake (CAN), McArthur River (CAN), Ranger (AUS), Jabiluka (AUS), Nabarlek (AUS)	Olympic Dam (AUS), Mt Painter (AUS)
Grades	Low to very high (0.04 to 22.28% U_3O_8)	Very low to low (0.05–0.1% U_3O_8)
Tonnages	Small to very large (up to 192,085 t U_3O_8)	Small to very large (up to 1,400,000 t U_3O_8)
Economic significance	Account for c. 20% of Australia's and 33% of the global U resources, and c. 29% of the global U production	Account for 65.5% of Australia's and 26% of the global U resources; Olympic Dam is the world's largest U deposit
Assigned uranium systems model	Unconformity-related systems	Igneous-related systems
Critical source processes	Leaching of U from: (1) enriched country/basement rocks; (2) enriched intrabasinal rocks; or (3) palaeo-regolith at unconformity	(1) Leaching of U from enriched country/basement rocks; or (2) expulsion of U-rich fluids from primary magmatic source (e.g., from suitable causative intrusions such as oxidized, magnetite-series granites)
Critical transport processes	(1) Transport of U in basinal brines; (2) migration of U-bearing fluids/brines via permeable strata, structures and/or unconformity surfaces (in particular fault–fault and fault–unconformity intersections)	(1) Transport of U in oxidized meteoric waters; (2) migration of U-bearing fluids via (preferably extensive, crustal-scale) fault networks (e.g., conjugate NW–SE and NE–SW structures in the Olympic Dam area)
Critical trap processes	(1) Creation of dilational sites by reactivation of long-lived crustal-scale structures; (2) space creation along fault surfaces and by extensive dissolution of quartz in sandstones	(1) Space creation by progressive, polyphase hydrothermal brecciation (e.g., caused by hydraulic, phreatic fracturing, dike injection and related phreatomagmatic explosions, faulting, gravitational collapse, chemical corrosion and/or subaerial eruptions) and alteration (e.g., hematite breccia complex at Olympic Dam) and associated weakening of the country rock
Critical deposition processes	(1) Mixing of oxidized, U-bearing brines and reduced, basement-derived fluids (i.e., meteoric model); or (2) interaction between oxidized U-bearing brines and reduced wallrocks (i.e., diagentic model)	Mixing of deep-seated brines and (1) U-bearing meteoric waters, and/or (2) magmatic fluids
Geological setting/characteristics	(1) Intracratonic basins with thick, permeable sandstone sequences that unconformably overlie crystalline basement; (2) fertile basins commenly recorded multiple high- to low-temperature fluid migration events and contain hydrocarbon accumulations	(1) Extensional intracratonic rift environments; (2) high-level intrusions in maar volcano-type settings; (3) evidence for significant and long-lived thermal events
Structure/architecture	(1) Major unconformities; (2) crustal-scale fractures; (3) structural complexity; (4) evidence for fault reactivation (e.g., variable sandstone thickness)	(1) Network of syn- to postmagmatic conjugate contractional structures with localised dilational zones (e.g., at Olympic Dam); (2) continuum of igneous to hydrothermal breccia types (e.g., hematite–granite to hematite–quartz breccia at Olympic Dam)
Alteration	(1) Alteration may extend up to 1 km, or more, from the mineralisation; (2) commonly sericite–chlorite ± kaolinite ± hematite assemblages; (3) Mg-metasomatism (and Mg-rich chlorite) is common; (4) strong desilicification at the unconformity and silification at higher stratigraphic levels where quartz is deposited in veins	(1) Complex, intense, laterally and vertically extensive and zoned alteration; (2) general trend from sodic alteration at deep levels, to potassic alteration at intermediate to shallow levels, to sericitic (hydrolytic) alteration and silicification at very shallow levels; (3) early magnetite alteration is commonly overprinted by intense iron-rich hematite alteration
Main mineralisation age	Proterozoic	Proterozoic
Relevant public-domain data (see Table 2)	Geological and tectonic maps and data (e.g., relatively undeformed sandstone sequences), structural data (e.g., faults, unconformities), geochemical data (e.g., composition and U content of basin sequences), redox potential (e.g., graphitic basement rocks or shear zones), depth-to-basement data, geophysical data (radiometrics, magnetics, gravity) (e.g., basin architecture), U occurrences, literature	Geological and tectonic maps and data (e.g., igneous provinces), structural data (e.g., caldera structures, hydrothermal and magmatic breccia occurrences), geochemical data (e.g., magma compositions), geophysical data (radiometrics, magnetics, gravity) (e.g., fault density, gravity and magnetic boundaries, uranium source regions), remote sensing data (e.g., caldera structures), U and other mineral (e.g., Cu-, Mo- and F-bearing) occurrences, literature

Sources: 1 = Dahlkamp (1978), Wilde and Wall (1987), Jackson and Andrew (1990), Mernagh et al. (1998), McKay and Miezitis (2001), Hein (2002), Lally and Bajwah (2006), Wall (2006), Jefferson et al. (2007), Pana et al. (2007); 2 = Australian Uranium Association (www.aua.org.au), Dahlkamp (1993), Gow et al. (1994), Haynes et al. (1995), Hitzman (2000), McKay and Miezitis (2001), Goad et al. (2001), Skirrow and Walshe (2002), Williams and Pollard (2003), Williams et al. (2005), Hitzman and Valenta (2005), Heinson et al. (2006).

to data collection and analysis; and (5) by focusing on critical processes that must occur to form a deposit, it can be linked to concepts of probability that allow for more meaningful and robust relative ranking of targets.

The aim of this study was to produce flexible models that are process-based, integrate information from a variety of sources, and emphasize the parameters that control the spatial and temporal distributions of uranium deposits at various scales. Based on these

Fig. 2. (a) The uranium classification scheme of the International Atomic Energy Agency (2000), illustrating the diversity of uranium deposit types and sub-types. Key to abbreviations: IAEA = International Atomic Energy Agency. (b) Comparison of the uranium classification scheme of the International Atomic Energy Agency (2000) and the uranium systems classification scheme proposed in this paper. In this new scheme, uranium deposit types are grouped according to similar genetic processes, environments of ore formation and mappable ingredients (i.e., exploration proxies or criteria) synthesized in Fig. 3 and Tables 1a–1e.

Table 1b

Volcanic[3]	Intrusion[4]	Surficial[5]
Streltsovskoye (RUS), McDermitt<(US), Ben Lomond (AUS), Pena Blanca (MEX), Macusani (PER)	Rössing (NAM), Ilimaussaq (GRE), Palabora (ZA), Radium Hill (AUS)	Yeelirrie (AUS), Lake Way (AUS), Lake Maitland (AUS), Langer Heinrich (NAM)
Low (0.02 to 0.29% U_3O_8)	Low (0.05 to 0.9% U_3O_8)	Low (0.02 to 0.24% U_3O_8)
Low to moderate; however, the Streltsovskoye deposit cluster has a large combined tonnage of 250,000 t U_3O_8	Small to large (up to 130,000 t U_3O_8)	Small to large (up to 52,500 t U_3O_8)
Account for 0.6% of Australia's U resources	Account for 0.3% of Australia's U resources; Rössing accounted for 7.7% of the global U production in 2005	Acount for 4.9% of Australia's uranium resources
Igneous-related	Igneous-related	Surficial systems
(1) Melting of U-rich sources (magmatic model); or (2) leaching of U from volcanic (in particular glass-rich ignimbrites and volcanic ash flows) and magmatic rocks (hydrothermal model)	(1) Mantle degassing; (2) melting of U-rich mantle/crustal source; or (3) leaching/scavenging of U from enriched country rocks by melts or magmatic fluids	(1) Leaching of U and K from (commonly intrusive or metamorphic) country rocks; and (2) supply of V from mafic- to ultramafic rocks or the regolith (V source is cryptic)
(1) Fractional crystallisation and volatile enrichment in magmas and/or expulsion of U-bearing magmatic fluids (magmatic model); or (2) U transport by oxidized hydrothermal fluids along permeable faults and unconformities (hydrothermal model)	(1) U enrichment in melts via fractional crystallisation (magmatic fractionation) and pervasive metasomatism, before and during magma ascent; (2) volatile exsolution (e.g., magmatic fluids)	(1) Transport of U in oxidized surficial and ground waters; and (2) focussing of fluid flow into aquifers (i.e., calcretes)
(1) Ground preparation (redox and competency gradients through juxtaposition of rocks with different chemical and physical make-ups); and (2) creation of depositional sites through dilational deformation and brecciation	(1) Enhanced heat flow, dilational deformation, permeability and suction focused on intrusions; (2) focusing of the volatile phase into faults or shear zones that are being actively deformed	Development of (1) porous calcrete accumulations in paleochannels and at playa lake margins; and (2) barriers within the aquifers that promote stagnation, pooling, drawing up and eventually evaporation of U-bearing groundwaters
(1) Fluid–wallrock interaction/fluid mixing(?)/ pressure changes(?) in faults, shear zones and breccias (discordant deposits); or (2) interaction between oxidized hydrothermal fluids and reduced mineral assemblages (stratabound deposits)	(1) Pressure and temperature decrease (promote magma cooling); (2) fluid–rock interaction; (3) fluid mixing; or (4) upgrading through hydrothermal alteration and/or weathering at surface (replacement of primary by secondary U minerals, and deposition of secondary U in fractures or newly created pore spaces)	(1) Changes in fluid chemistry due to evaporation and interaction between U-bearing fluids and calcium carbonate in the calcretized horizons; (2) adsorption of U onto clays
(1) Calderas with strong peralkaline affinities (Na + K>Al) in extensional(?) back-arc environments; (2) volcanic cauldron subsidence structures with co-magmatic granitic intrusions, ring dykes, ignimbrites, pyroclastic rocks and intra-caldera volcaniclastic rocks; (3) caldera-related volcanogenic facies near calderas	Metamorphic belts with abundant granite and pegmatite that mark former active continental margin environments	(1) Stable cratonic environments with extensive palaeodrainage systems and playa lakes; (2) U-, K- and V-enriched hinterland, bedrock or regolith; (3) arid to semi-arid climatic conditions characterized by intermittent rainfall and high evaporation rates; (4) poor preservation potential of these surficial drainages means that younger systems are the more preferable exploration targets
(1) Discordant deposits: shear zone- and fault-hosted veins, dykes and diatremes; (2) stratabound deposits: porous and permeable volcanogenic rocks	Major crustal breaks that served as magma conduits; all known igneous U provinces recorded low-angle (<30°) subduction	
Albitization, carbonatization, argillization, silicification, chloritization, hematization	Regional metasomatism	
Paleozoic to Cenozoic	Proterozoic to Mesozoic	Cenozoic
Refer to data in breccia complex column	Refer to data in breccia complex column	Geological and tectonic maps and data (e.g., calcrete provinces, karsted limestone provinces), geochemical data (e.g., V content of mafic rocks), redox potential, hydrological data (e.g., flow directions, groundwater salinities), geophysical data (radiometrics, magnetics, gravity) (e.g., paleochannels, U source regions), remote sensing data (e.g., collapse structures, playa lakes, paleochannels), U and V occurrences, (palaeo-)climate data, literature

Sources: 3 = Australian Uranium Association (www.aua.org.au), Dahlkamp (1978), McKay and Miezitis (2001), Chabiron et al. (2003), Vigar and Jones (2005); 4 = Parkin and Glasson (1954), Berning et al. (1976), Buntebarth (1976), Dahlkamp (1978), Ashley (1984), McKay and Miezitis (2001), Basson and Greenway (2004), Zhao et al. (2004); 5 = Langford (1974), Dahlkamp (1978), Mann and Deutscher (1978), Bowie (1979), Cameron et al. (1980), Butt et al. (1984), Hartleb (1988), Cameron (1990), McKay and Miezitis (2001), de Broekert and Sandiford (2005).

premises and applying a mineral systems approach, the 14 principal uranium deposit types recognized by the International Atomic Energy Agency (2000) (Fig. 2a) were grouped into six uranium systems models (Figs. 2b, 3): (1) surficial; (2) sedimentary; (3) igneous-related; (4) metamorphic/metasomatic; (5) unconformity-related; and (6) vein-related uranium systems. Each of these systems includes uranium deposit types that are characterized by similar genetic processes, environments of ore formation, and mappable criteria or exploration proxies (e.g., geological setting, age structure and alteration: cf. Tables 1a–1e).

Table 1c

Collapse breccia pipe[6]	Metasomatite[7]	Metamorphic[8]
Orphan Lode (US), EZ-2 (US), Pigeon (US), Sanbaqi (CHI)	Valhalla (AUS), Skal (AUS), Ross Adams (US), Lagoa Real (BRA), Espinharas (BRA), Zheltye Vody (UKR)	Mary Kathleen (AUS)
Medium to high (0.4 to 1% U_3O_8)	Low (0.13 to 0.16% U_3O_8)	Very low to low (0.001 to 0.15% U_3O_8)
Small to moderate (up to 15,000 t U_3O_8)	Small to moderate (up to c. 30,000 t U_3O_8)	Small to moderate (up to 9,200 t U_3O_8)
No Australian examples; relatively high grades mean that these deposits can be mined profitably despite their relatively small size	Account for 1.5% of Australia's U resources	Account for 0.1% of Australia's U resources
Surficial	Metamorphic/metasomatic	Metamorphic/metasomatic
Leaching of U from volcanic rocks and ash deposits exposed at or near surface	(1) Leaching of U from enriched (commonly intrusive and volcano–sedimentary) country rocks; or (2) expulsion of U-bearing fluids from primary magmatic sources	Leaching of U from enriched (commonly metamorphic or magmatic) country rocks during regional metamorphism and/or contact metamorphism
(1) Transport of U by oxidized, saline waters via aquifers; and (2) focussing of fluid flow into permeable collapse breccia pipes due to elevated hydraulic gradients	(1) Transport of U by oxidized hydrothermal fluids; and (2) fluid migration along permeable shear zones and/or faults and unconformities	Transport of U by metamorphic fluids
(1) Creation of permeability through brecciation of sedimentary and volcanic sequences and collapse into pipe-like dolines that formed in underlying karsted limestone sequences; (2) sulfide accumulations and impregnations form redox boundaries within and in the wallrocks of permeable collapse breccia pipes	(1) Ground preparation via introduction of a reduced mineral assemblages (e.g., chlorite) in country rocks affected by regional metasomatism; (2) creation of structural permeability during regional deformation	(1) Ground preparation via metasomatism and contact metamorphism prior to U mineralization; (2) deformation-induced brecciation and creation of dilational sites along faults and shear zones
Interaction between oxidized, saline, metal-rich fluids and strongly reduced wallrocks and wallrock fragments within the solution collapse breccia fill	Interaction of oxidized U-bearing fluids with a reduced mineral assemblage (e.g., chlorite, hornblende, epidote) and/or carbonaceous rocks	Fluid–rock interaction
Stable marine platforms where platform carbonates and carbonate-cemented sandstones were subjected to repeated upward stoping and karsting	Multiply deformed metamorphic belts (preferably former intracratonic rift basins) that were affected by regional metasomatism	Metamorphic belts with long histories of fluid–rock interaction, protracted thermal events and formation of skarns and contact metamorphism around granites
(1) Collapse breccia pipes are near-vertical cylindrical pipes with diameters of up to 175 m and vertical extents of up to 1,000 m; (2) concealed pipes are often marked by surface depressions and accompanied by ring fracture zones; (3) U mineralization is commonly overlain by a 'massive sulphide cap' consisting of pyrite, marcasite and base-metal sulphides	Strong structural control but no detailed information available	Strong structural control but no detailed information available
(1) Silification, reduction-related bleaching; (2) carbonate, sulphate, kaolinite, chlorite, sericite	(1) Regional sodic metasomatism (Na_2O enrichment, SiO_2 depletion); (2) intense carbonate and hematite alteration	Garnet, diopside, scapolite and albite
Paleozoic to Mesozoic	Proterozoic	Proterozoic
Refer to data in surficial column	Geological and tectonic maps and data (e.g., metamorphosed or metasomatised rock packages), structural data (e.g., faults, shear zones), geochemical data (e.g., Na, K and Ca metasomatism), redox potential (e.g., reduced strata), geophysical data (radiometrics, magnetics, gravity) (e.g., fault density, U source regions), U occurrences, literature (e.g., intrusive and metamorphic events)	Refer to data in metasomatite column

Sources: 6 = Wenrich (1985, 1986), Van Gosen and Wenrich (1989), Finch (1992), Min et al. (1997), McKay and Miezitis (2001), Wenrich et al. (2004); 7 = Dahlkamp (1978), McKay and Miezitis (2001), Gregory et al. (2005), Duncan et al. (2006); 8 = Bowie (1979), Heier (1979), Ahmad and Wilson (1981), Cartwright (1994), Gregory et al. (2005), Marshall et al. (2006), McKay and Miezitis (2001), Oliver et al. (1999).

2.3. GIS database

The quality, resolution and scope (e.g., outcrop versus bedrock geology maps) of digital datasets publicly available in Australia vary from state to state, but most data can be considered accurate and complete at the scale of this study and, therefore, provided an excellent foundation for the prospectivity analysis. Table 2 lists the databases that were used in this study.

2.4. Scope, design, conduct and results of the prospectivity analysis

This prospectivity analysis was undertaken at the geological region level for all states and territories of Australia that allow uranium exploration, namely, the Northern Territory, Queensland, South Australia, Tasmania and Western Australia. A geological region is defined by Geoscience Australia (Bain and Draper, 1997; www.ga.gov.au/meta/ANZCW0703002397.html) as geographical area with a cohesive geological assemblage that is significantly different in overall geology from the adjoining regions, and differs from a geological province in that it does not include depth and time dimensions. Geological regions are commonly used by Geoscience Australia as the geological units for assessments (e.g., Skirrow, 2009) and geological reference for minerals and resources mapping products (e.g., McKay et al., 2009; Schofield, 2009b,c,d). Given the above, geological regions were selected as the units and geological reference framework for this prospectivity analysis. Overall, the study area covers 90 of the 100 geological regions (Fig. 4a–b) and approximately 87% of the total area of the Australian continent.

In the analysis, each of the 90 geological regions was assessed and ranked in terms of (1) its probability of occurrence of surficial,

Table 1d

Sandstone[9]	Quartz–pebble conglomerate[10]	Phosphorite[11]
Inkai (KAZ), Muyunkum (KAZ), Arlit (NIG), Smith Ranch (US), Beverley (AUS), Honeymoon (AUS)	Witwatersrand (ZA), Elliot Lake (CAN)	Florida Phosphorite Province (US), Phosphoria Basin (US), Duchess (AUS), Phosphate Hill (AUS)
Low to medium (0.05 to 0.4% U_3O_8)	Low (0.04 to 0.1% U_3O_8)	Low (0.01 to 0.3% U_3O_8)
Australia: small to moderate (up to 17,600 t U_3O_8); elsewhere: small to large (up to 122,000 t U_3O_8)	Large (up to 200,000 t U_3O_8)	Moderate to large (up to 270,000 t U_3O_8)
Account for 6.7% of Australia's and 19% of global U resources	Account for 4% of global U resources No known economic examples in Australia	U is a byproduct of the phosphate mining process No U is extracted from any of the phosphate mines operating in Australia
Amenable to low-cost in-situ leach recovery (ISR)		
Sedimentary	Sedimentary	Sedimentary
Leaching of U from: (1) enriched (commonly intrusive and metamorphic) country rocks; (2) enriched (commonly tuffaceous or sedimentary) rocks interbedded with or overlying sandstones; or (3) existing U concentrations	(1) Erosion of exposed U source rocks under reduced atmospheric conditions prior to c. 2.2 Ga (paleoplacer model); or (2) leaching of U from source rocks in the basement or basin (hydrothermal model)	Leaching or erosion of U from: (1) enriched terrestrial source rocks (e.g., granites); or (2) reworked marine sediments
(1) Transport of U in oxidized surficial and ground waters; (2) fluid migration along aquifers and/or permeable faults	(1) Fluvial transport of detrital uraninite grains under anoxic atmospheric conditions (paleoplacer model); or (2) transport of U by meteoric waters and along fractures and faults that postdate deposition of the host conglomerates (hydrothermal model)	Transport of U by: (1) surficial waters (rivers); and/or (2) ocean currents (influenced by topography, climate and prevailing winds)
Local and regional redox boundaries	(1) Physical and chemical traps (e.g., mats of cyanobacteria) within alluvial fan environments (paleoplacer model); or (2) intraformational unconformities, geological contacts, carbonaceous seams (hydrothermal model)	(1) Topographic features (e.g., local highs and troughs); (2) pockets of reduced water on the sea floor; (3) release of phosphate due to bacterial transformation of organic matter
(1) Interaction between U-bearing oxidized fluids and carbonaceous matter or reducing agents (e.g., pyrite, hydrocarbons, vanadiferous clays); (2) upgrading through mobilisation of previously adsorbed U, and redeposition and concentration of the mobilised U ahead of the redox front	(1) Gravitational sorting and concentration (paleoplacer model); or (2) fluid mixing and/or fluid wallrock interaction (e.g., U concentration along thin carbonaceous seams) (hydrothermal model)	(1) Phosphogenesis (whereby U is concentrated in the carbonate fluorapatite mineral francolite); (2) U upgrading through reworking and concentration of phosphate during subsequent marine transgressions, supergene enrichment of phosphate by interaction with acid ground waters or mobilisation of phosphate at the base of the weathered zone
(1) Intracratonic basins, in particular alluvial fan environments, intermontane basins and marine/non-marine coastal plains within such basins; (2) stable cratonic environments with incised palaeodrainage systems; (3) greater number of post-Silurian occurrences possibly linked to post-Silurian onset of widespread vegetation cover	(1) Continental rift basins comprising alluvial fan and/or braided river environments; (2) submature to mature, cross-bedded polymict conglomerates and arkoses; (3) Witwatersrand-type: U-bearing conglomerate horizons occur along deformed intraformational unconformities; (4) Huronian-type (e.g., Elliot Lake): U-bearing conlomerates occur at the base of the Huronian Supergroup; (5) temporal distribution possibly restricted to the Archean and early Paleoproterozoic due to oxidation of Earth's atmosphere from c. 2.2 Ga	(1) Tectonically stable, shallow (restricted) continental shelf environments with local highs and troughs; (2) areas of warm water, low rates of detrital sedimentation and slightly reducing conditions; (3) phosphate-rich, shallow-marine sedimentary rocks
Permeable fault zones important in the genesis of structurally controlled deposits; mineralization is commonly stratabound and stratiform	Mineralization is stratiform/stratabound; Witwatersrand-type: strong structural control on mineralization (regional scale: normal faults, deposit scale: bedding-parallel shears and thrusts), evidence for remobilisation of uranium and gold; Huronian-type: strong evidence for sedimentological controls (decreasing pebble size and change in ore composition with increasing distance from inferred source)	Mineralization is stratabound and stratiform
Alteration and mineralization sequence for rollfront-type U deposits (from oxidized to reduced sandstone): (1) hematitic core (hematite, magnetite, kaolinite); (2) limonitic front (siderite, goethite, kaolinite); (3) U ore; and (4) proto-ore (molybdenite, pyrite, jordisite, calcite, hydrocarbon)	Witwatersrand-type: muscovite, chlorite, pyrophyllite, chloritoid, quartz, rutile, pyrite	U bound in francolite
Mainly post-Silurian	Archean to early Paleoproterozoic	Proterozoic to Cenozoic
Geological and tectonic maps and data (e.g., black shale provinces), structural data (e.g., faults, folds, unconformities), geochemical data (e.g., composition of and U content of sedimentary sequences), depth-to-basement data, redox potential (e.g., reduced strata), geophysical data (radiometrics, magnetics, gravity) (e.g., basin architecture, U source regions), remote sensing data (e.g., thermal imagery for delineation of palaeochannels), U occurrences, other relevant natural resource occurrences (e.g., coal, lignite, phosphate, oil and gas), literature	Refer to data in sandstone column	Refer to data in sandstone column

Sources: 9 = Bowie (1979), Dahlkamp (1978, 1993), Finch and Davis (1985), Hobday and Galloway (1999), McKay and Miezitis (2001), Brugger et al. (2005), Spirakis (1996); 10 = Bowie (1979), Sanford (1990), Vennemann et al. (1992), Dahlkamp (1993), Coward et al. (1995), Spirakis (1996), Hobday and Galloway (1999), McKay and Miezitis (2001), England et al. (2002), Frimmel (2005), Law and Phillips (2006), Wall (2006); 11 = Altschuler et al. (1958), Bowie (1979), Howard and Hough (1979), Finch (1996), Solomon and Groves (2000), McKay and Miezitis (2001).

Table 1e

Lignite[12]	Black shale[13]	Vein[14]
Lignite Basin (US), Serres Graben (GRE), Ebro Valley (ESP), Mulga Rock (AUS)	Ranstad (SWE), Ronneburg (GER), Chattanooga Shale (US)	Schwartzwalder (US), Krunkelbach (GER), Streltsovskoe (RUS), Twin and Dam (AUS)
Very low to low (0.005 to 0.2% U_3O_8)	Very low to low (0.005 to 0.17% U_3O_8)	Low to high (0.1 to 2.4% U_3O_8)
Small to moderate (up to 16,531 t U_3O_8; however, deposit clusters can contain large combined tonnages of up to 200,000 t U_3O_8)	Large to very large (up to 4,000,000 t U_3O_8)	Small to moderate (up to 24,000 t U_3O_8)
Grades commonly too low for commercial extraction; Mulga Rock is likely commercially viable but its classification is controversial	Very large resource base but currently not economic to mine due to technical challenges of U extraction from black shales	Account for c. 1% of global uranium resources; Commonly narrow and structurally complex
Sedimentary	Sedimentary	Vein-related
Leaching of U from enriched source rocks (e.g., lamproites, kimberlites or carbonatites, granitic and metamorphic rocks, volcanic rocks and ash)	Leaching of U from enriched source rocks (commonly granites)	Leaching of U from: (1) enriched (commonly igneous and metamorphic) country rocks; or (2) paleo-regolith (at unconformity surfaces)
(1) Transport of U by oxidized, saline groundwaters; (2) topography-driven groundwater flow through aquifers and permeable structures; (3) paleodrainage systems	Transport of U into ocean basins by oxidized surficial waters (e.g., rivers)	(1) Transport of U by oxidized hydrothermal or meteoric fluids; (2) fluid migration along permeable shear zones and/or faults
Redox boundaries (i.e., boundary between organic-rich peat and lignite beds and oxidized sedimentary sequences)	Black shales in epicontinental basins	(1) Strong structural control on ore deposition at all scales; (2) ground preparation during previous deformation and thermal events; (3) dilational zones next to/near major fault or shear zones; (4) redox gradients
(1) Reduction and deposition of U at redox interfaces (i.e., reduced lignite/oxidized sediments within aquifers) and adsorption onto peaty clay particles; (2) upgrading through remobilization of previously adsorbed U, and redeposition and concentration of this remobilised U	(1) Reduction of U by organic matter and pyrite in black shales; (2) adsorption of U onto organic material and clay minerals in black shales	(1) Effervescence; (2) fluid mixing; or (3) fluid–rock interaction
(1) Intramontane and/or intracratonic basin and graben environments that received large amounts of clastic sediments from a U-enriched hinterland and organic matter; (2) stable cratonic environments with incised palaeodrainage systems	(1) Tectonically stable terranes characterized by low sedimentation rates, brackish to normal marine salinities, anaerobic, strongly reducing conditions; (2) shallow, partially closed (barred) epicontinental basin environments; (3) laminated black shales that are very fine-grained and characterized by high organic and sulphide contents	Metamorphic belts (i.e., postorogenic cratonic environments), preferably with calc-alkaline felsic plutonic and volcanic rocks that are cut by major fault and shear zones
(1) Permeable fault zones important in the genesis of structurally controlled deposits; (2) mineralization is commonly stratabound and stratiform	Mineralization is stratabound and uniformly disseminated	Breccia zones, faults, shear zones
No information	Sericite, chlorite ± fluorite in the case of shales having been hydrothermally overprinted	(1) Sericite, chlorite ± hematite ± apatite; (2) carbonate, sericite; (3) hematite, adularia
Cenozoic	Precambrian to recent	Proterozoic to Mesozoic(?)
Refer to data in sandstone column	Refer to data in sandstone column	Geological and tectonic maps and data (e.g., orogenic provinces), structural data (e.g., fault density), geochemical data (e.g., U content of potential host rocks), redox potential, geophysical data (radiometrics, magnetics, gravity, gravity and magnetic boundaries, U source regions), remote sensing data, U occurrences, literature (e.g., intrusive and metamorphic events)

Sources: 12 = Dahlkamp (1978), Bowie (1979), Psilovikos and Karistineos (1986), Fulwood and Barwick (1990), Georgakopoulos (2001), McKay and Miezitis (2001), Douglas et al. (2003); 13 = Bowie (1979), Allard et al. (1991), Lewan and Buchardt (1989), Dahlkamp (1993), Spirakis (1996), McKay and Miezitis (2001), Langwaldt (2006); 14 = Dahlkamp (1978), Ludwig et al. (1985), Wallace and Karlson (1985), Wallace and Whelan (1986), Hofmann and Eikenberg (1991), Ruzicka (1993); McMillan (1996), McKay and Miezitis (2001).

sedimentary, igneous-related, metamorphic/metasomatic, unconformity-related, and vein-related uranium systems (Fig. 5a–f): i.e., technical ranking scheme; (2) its potential to host uranium deposits of sufficient grade and tonnage that are potentially mineable (Fig. 6a): i.e., quality ranking scheme; and (3) available ground for area selection (Fig. 6b): i.e., opportunity ranking scheme. The rationale for each ranking, assigned probability values, and results were recorded in a standardized prospectivity matrix, which served to promote objectivity, transparency and reproducibility. Tables 3a–3f provide excerpts of this matrix, using the Yilgarn, Musgrave, Eromanga, Carnarvon, Pine Creek and King Leopold regions as examples.

The technical ranking followed the approaches of Lord et al. (2001) and Kreuzer et al. (2008), which combine the mineral systems approach and aspects of probability theory into semi-quantitative models for evaluation and ranking of exploration projects. These approaches require the following actions: (1) formulation of underlying uranium systems models, including identification of the independent, critical processes of uranium deposit formation; (2) assignment of probabilities to each process factor; and (3) application of the multiplication rule to obtain an overall probability of potentially economic mineralization being present at the location of interest. In this study, the subjectively assessed probabilities of the critical processes of uranium deposit formation included: P_1 = probability of uranium extraction from potential sources (this includes processes that provide energy to drive a mineral system such as tectono-thermal events, and release fluids), P_2 = probability of transport of uranium from sources to traps, and P_3 = probability of uranium deposition. The probability of discharge of residual fluids or melts through outflow zones (i.e., P_4) is not considered here given the common lack of evidence for this process in regional-scale datasets and loss of affected stratigraphy because of erosion.

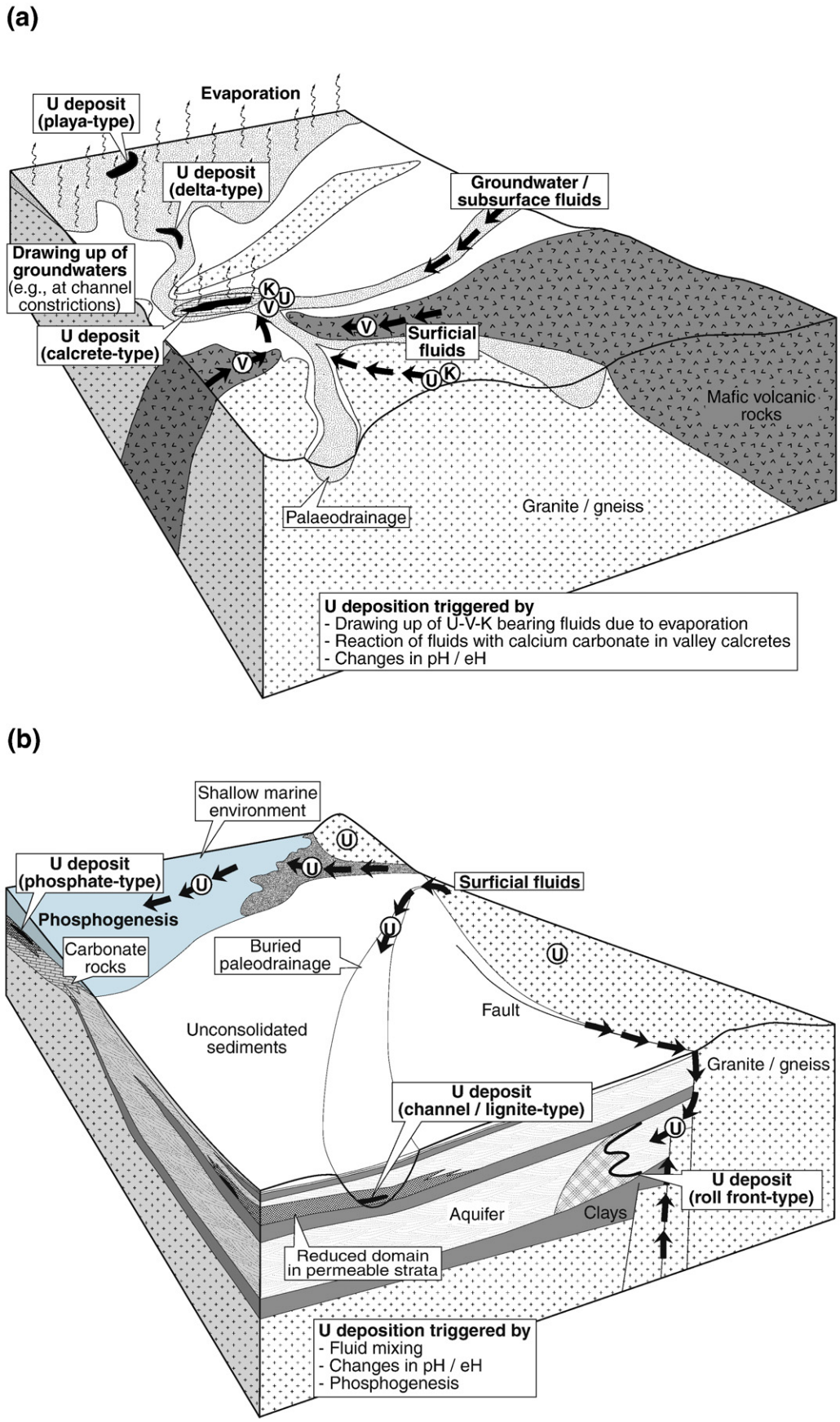

Fig. 3. Schematic representation of critical processes and essential ingredients in the formation for the six uranium systems that formed the basis of this continent-wide uranium prospectivity analysis. (a) Surficial uranium systems. (b) Sedimentary uranium systems. (c) Igneous-related uranium systems. (d) Metamorphic/metasomatic uranium systems. (e) Unconformity-related uranium systems. (f) Vein-related uranium systems. A list of the main characteristics, and essential ingredients and critical processes in the formation of these six uranium systems is given in Tables 1a–1e.

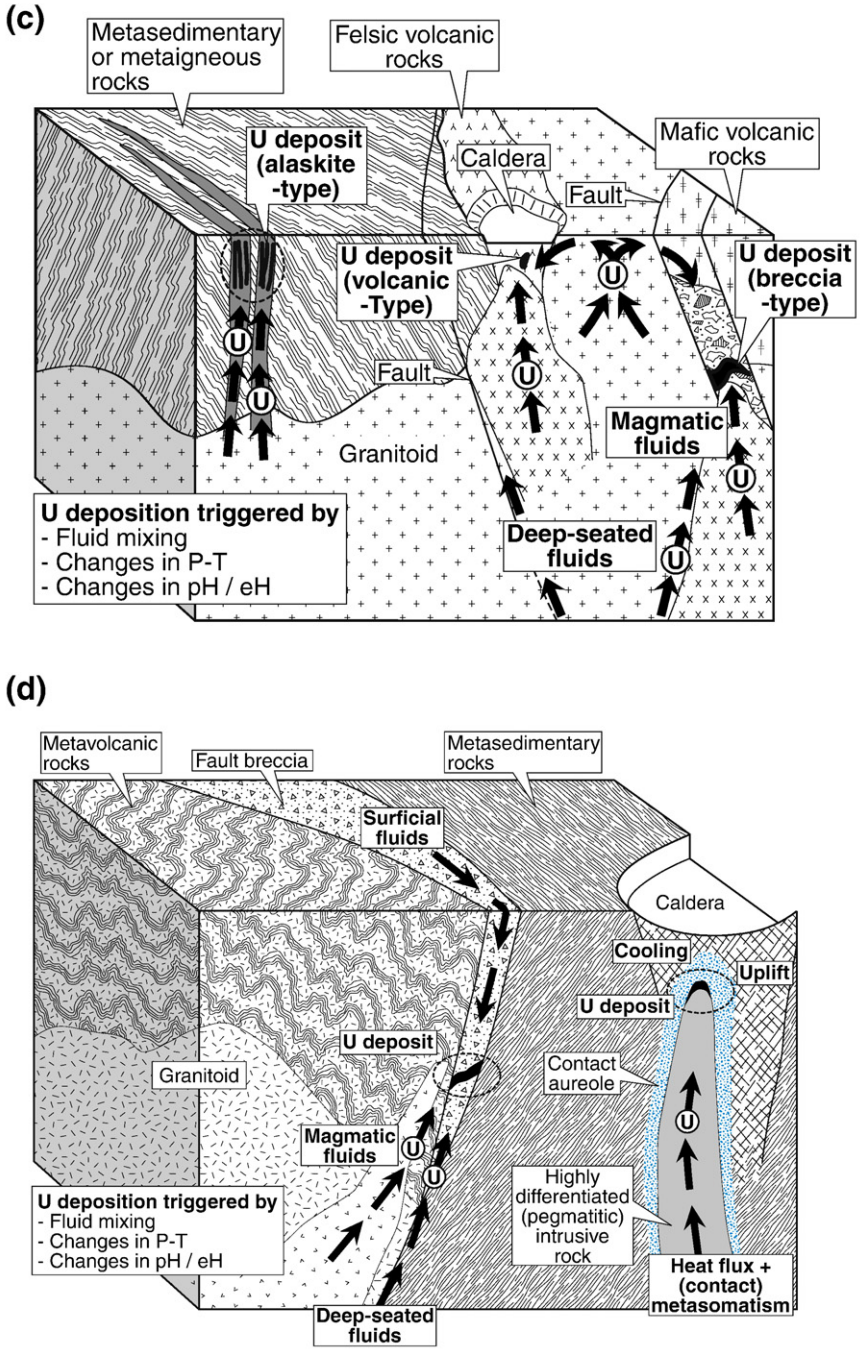

Fig. 3 (*continued*).

The assignment of probabilities to P_1 to P_3 was a team effort and all numbers represent a consensus (or mean) value of the probabilities assigned by each team member. The Sherman–Kent scale (e.g., Watson, 1998; Jones and Hillis, 2003) was used to calibrate, elicit and quantify individual judgments (Table 4). The probabilities of occurrence of the critical processes were multiplied to obtain an overall probability of occurrence of uranium mineralization (i.e., $P_{Mineralization} = P_1 \times P_2 \times P_3$) in each geological region. The $P_{Mineralization}$ values for the geological regions were mapped to generate a series of prospectivity maps (Fig. 5) that illustrate the relative uranium potential for each of the six uranium systems.

The quality ranking scheme accounts for differences between uranium systems in terms of their grade and tonnage, and mineability. In this scheme, the $P_{Mineralization}$ values of the technical ranking scheme were multiplied with a subjective quality factor, Q, that was defined based on likely grade-tonnage ranges (McKay and Miezitis, 2001; proprietary Mining Project database of Intierra Resource Intelligence; Thomas et al., 2006; uranium company websites) and mineability of the targeted deposit types (Table 5). This approach delivered a single prospectivity map (Fig. 6a), highlighting those geological regions with the greatest potential for high-quality uranium systems characterized by high grades, large tonnages and/or relatively low mining costs.

In the opportunity ranking scheme, each geological region was categorized based on the amount of ground available for pegging and

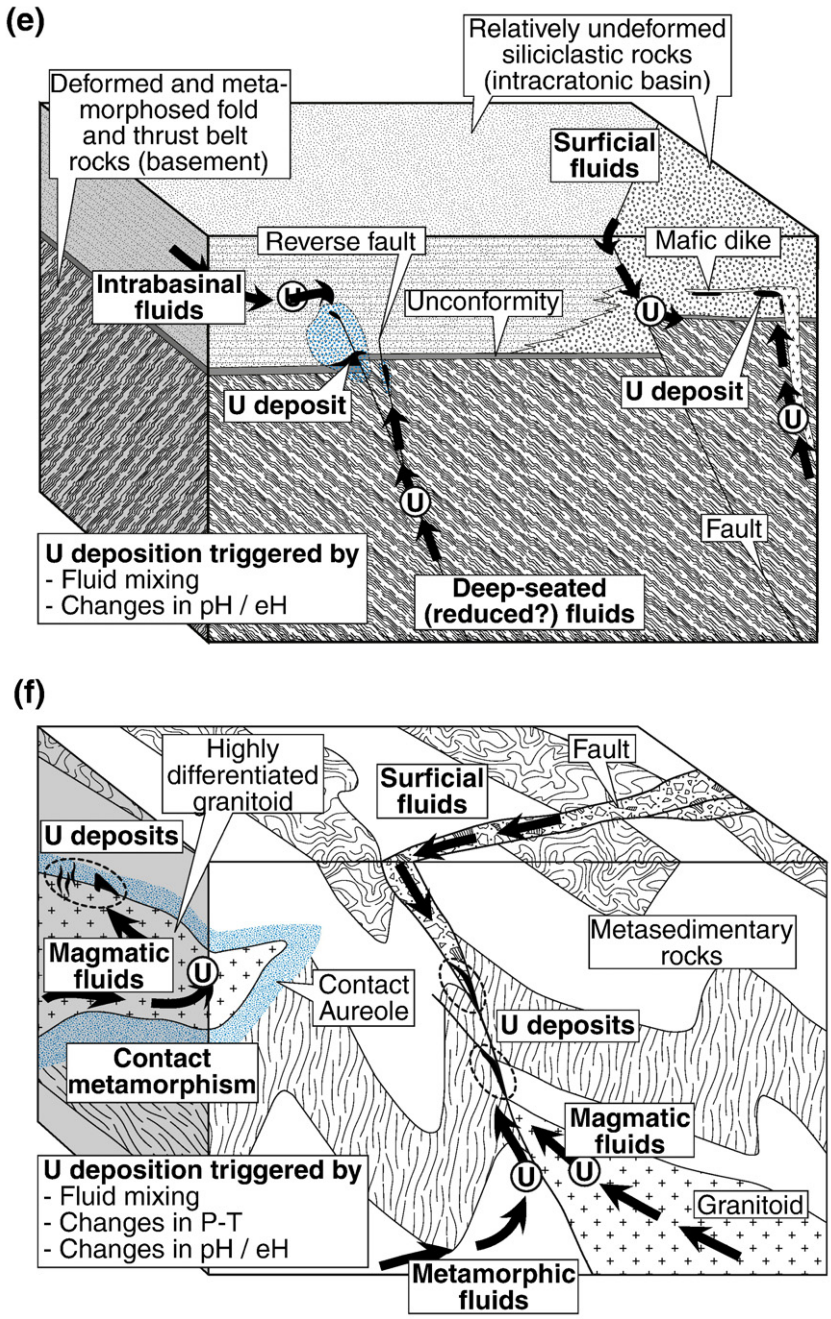

Fig. 3 (*continued*).

ranked on a scale from 1.0 (i.e., poor ground availability) to 4.0 (i.e., outstanding). The resulting opportunity map (Fig. 6b) was a useful tool for area prioritization and effective allocation of time and resources.

2.5. Identification and evaluation of uranium prospective ground

Vacant uranium prospective ground identified in the prospectivity analysis was subjected to more detailed follow-up study. Much of this ground was acquired by the company that sponsored the underlying uranium prospectivity analysis.

3. Case studies

The three case studies given below illustrate key procedures of the manual prospectivity analysis using surficial, sedimentary and unconformity-related uranium systems as examples (Tables 3a–3f). These systems were chosen given their common occurrence in Australia and global significance (cf. McKay and Miezitis, 2001). Each case study portrays two prospective geological regions: one that contains significant deposits of a particular uranium system and, therefore, is relatively data-rich with respect to this particular system; the other contains only minor occurrences or deposits of the particular uranium system, or none, and, therefore, is relatively data-poor. Data-rich and data-poor regions were selected to illustrate how data availability affects the prospectivity analysis and how probability values assigned to P_1 to P_3 can be used to account for geological uncertainties linked to data inadequacy. The processes and sub-processes critical in the formation of the various uranium systems and underlying this assessment are summarized in Fig. 3 and Tables 1a–1e.

Table 2
Precompetitive data utilized in this study and their sources.

Theme	Type of data	Purpose and derivative data	Source(s)
Geography/topography	Drainage	First-order drainage systems served as a proxy for paleodrainage systems	GA
	Waterbodies	Location of playa lakes	GA
	Road	Geographic reference; general land use	GA
	Rail	Geographic reference; general land use	GA
	Localities	Geographic reference; general land use	GA
	NATMAP topographic maps	Geographic reference; topographic information; general land use	GA
Climate	Climate maps and data	Annual averages and seasonal data served as proxy for late Tertiary to early Quaternary climate	BOM
	Literature	Tertiary to Quarternary paleoclimate information	Various
Geology	Australian crustal elements	Tectonic framework of the Australian continent	GA
	Geological regions	Boundaries and brief geological summaries of the regions that were analyzed in this study GA	
	Geology	Geological reference and information	DME, GA, GSWA, MRT, NTGS, PIRSA
	Regolith	Served to extract mappable ingredients of calcrete-hosted uranium systems (calcrete occurrences, alluvial sediments, playa lake sediments); outcrop locations served to evaluate interpreted palaeodrainage systems	GSWA
	Paleodrainage map	Potential pathways for uranium-bearing ground waters	PIRSA
	Faults	Potential fluid pathways and structural controls	DME, GA, GSWA, MRT, NTGS, PIRSA
	Folds	Potential fluid pathways and structural controls	GA
	Crustal breaks	Potential fluid pathways and structural controls; crustal-scale faults	GA
	Crustal thickness	Proxy for regions of higher heat flow, which has implications for basin maturation	GA
	Sediment thickness	Depth to uranium prospective basement under cover; information about the thickness and potential fertility of sedimentary basins	GA
	SEEBASE™ (depth-to-basement model)	Depth to uranium prospective basement under cover; information about the thickness and potential fertility of sedimentary basins	FrOG Tech
Uranium occurrences	MINLOC (mineral localities database)	Location of uranium deposits and occurrences	GA
	Minmet Global	Location of uranium deposits and occurrences; grade-tonnage data	Intierra Resource Intelligence
Geochemistry	OZCHEM (national whole rock geochemistry data)	Delineation of domains of uranium enrichment (defined here as >15 ppm U) and vanadium enrichment (defined here as >100 ppm V)	GA
Geophysics	Gamma-ray spectrometry data	Delineation of potential uranium source regions; domains of uranium enrichment	DME, GADDS, GSWA, NTGS, PIRSA
	Magnetic data	Delineation of the subsurface extent of intrusive and metamorphic complexes that are known to be uranium enriched and complexes that are not exposed but possibly enriched	DME, GADDS, GSWA, NTGS, PIRSA
	Gravity data	Delineation of the subsurface extent of intrusive and metamorphic complexes that are known to be uranium enriched and complexes that are not exposed but possibly enriched	DME, GADDS, GSWA, NTGS, PIRSA
Remote sensing	AVHRR (Advanced Very High Resolution Radiometer)	Delineation of potential paleodrainage systems	NOAA
	LandSat	Topographic information	GA
	DEM (Digital elevation model)	Definition of first-order drainage channels, which served as proxies for paleodrainage systems	GA
Heat flow	Crustal heat flow at 5 km depth	Delineation of potential sources of uranium enrichment in the crust	GA
Exploration	Australian land tenure	General land use; public, private and indigenous lands	GA
	Exploration and mining licenses	Mineral exploration and mining tenure	DME, GSWA, MRT, NTGS, PIRSA
	Company data	Geological information and concepts; resource data	ASX, Company Websites
	Literature	Geological information and concepts; resource data	Various

Key to abbreviations: ASX = Australian Securities Exchange; BOM = Bureau of Meteorology; DME = Department of Mines and Energy Queensland; FrOG Tech = FrOG Tech - From Oil to Groundwater; GA = Geoscience Australia; GADDS = Geophysical Archive Data Delivery System; GSWA = Geological Survey of Western Australia; MRT = Mineral Resources Tasmania; NOAA = National Oceanic and Atmospheric Administration; NTGS = Northern Territory Geological Survey; PIRSA = Department of Primary Industries and Resources of South Australia.

3.1. Surficial uranium systems

3.1.1. Yilgarn Region (Western Australia)

The Yilgarn Region (Fig. 4b) covers an area of 624,000 km^2. The main geological element within this region is the Yilgarn Craton, one of the largest intact segments of Archaean crust on Earth (Anand and Paine, 2002). The Yilgarn Craton is a typical metamorphosed granite–greenstone terrain with arcuate belts of sedimentary and volcanic rock (i.e., greenstones) that are enclosed by large areas of granite and granitic gneiss. Most of the Archaean rocks of the craton formed between c. 3.05 and 2.62 Ga, with a minor older component (>3.7 Ga). Amalgamation between 2.78 and 2.63 Ga of the various terranes (Cassidy et al., 2006) that make up the Yilgarn Craton was marked by intense tectonic, igneous and metamorphic activity (Myers, 1993). Calcrete-hosted surficial uranium deposits of the Yilgarn Craton are spatially associated with an extensive fossil river system (Fig. 7) that has been superimposed on the Archaean basement and weathered land surface probably as early as the Jurassic (Anand and Paine, 2002; de Broekert and Sandiford, 2005). Early Tertiary rejuvenation of this river system produced a network of relatively narrow, incised

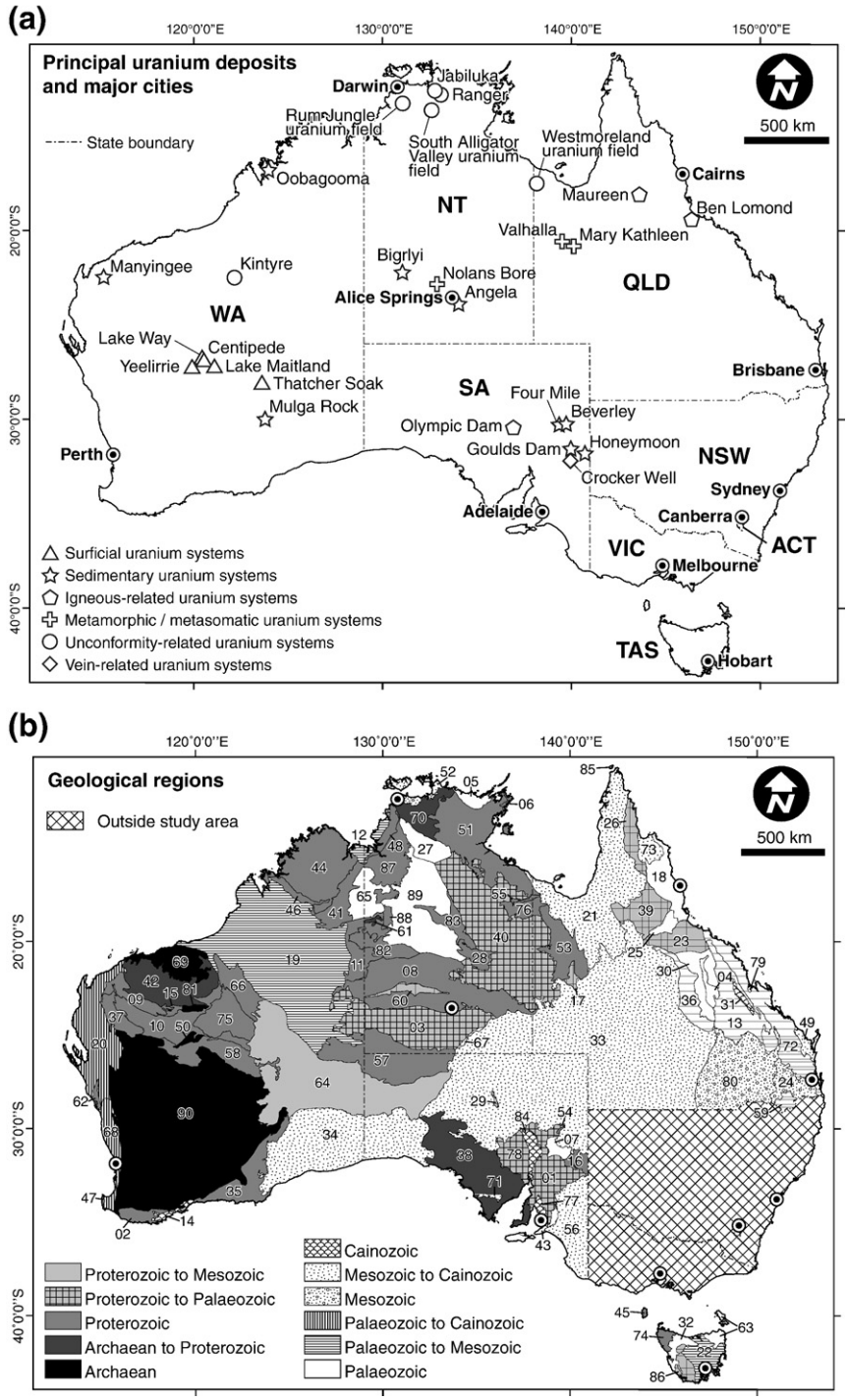

Fig. 4. (a) Map of the principal uranium deposits and fields in Australia, also illustrating the location of major cities and state boundaries. Key to abbreviations: ACT=Australian Capital Territory, NSW=New South Wales, NT=Northern Territory, QLD=Queensland, SA=South Australia, TAS=Tasmania, VIC=Victoria, WA=Western Australia (b) Map of the study area, which covered all states and territories except for New South Wales and Victoria (where uranium exploration and mining are currently not permitted) and included 90 geological regions of Australia: 01 = Adelaide, 02 = Albany, 03 = Amadeus, 04 = Anakie, 05 = Arafura, 06 = Arnhem, 07 = Arrowie, 08 = Arunta, 09 = Ashburton, 10 = Bangemall, 11 = Birrindudu, 12 = Bonaparte, 13 = Bowen, 14 = Bremer, 15 = Bresnahan, 16 = Broken Hill, 17 = Burke River, 18 = Cairns, 19 = Canning, 20 = Carnarvon, 21 = Carpentaria Lowlands, 22 = Central Tasmania, 23 = Charters Towers, 24 = Clarence-Moreton, 25 = Clarke River, 26 = Coen, 27 = Daly River, 28 = Davenport, 29 = Denison, 30 = Drummond, 31 = Duaringa, 32 = Dundas, 33 = Eromanga, 34 = Eucla, 35 = Fraser, 36 = Galilee, 37 = Gascoyne, 38 = Gawler, 39 = Georgetown, 40 = Georgina, 41 = Halls Creek, 42 = Hamersley, 43 = Kanmantoo, 44 = Kimberley, 45 = King Island, 46 = King Leopold, 47 = Leeuwin, 48 = Litchfield, 49 = Maryborough, 50 = Marymia, 51 = McArthur, 52 = Money Shoal, 53 = Mount Isa, 54 = Mount Painter, 55 = Murphy, 56 = Murray, 57 = Musgrave, 58 = Nabberu, 59 = New England, 60 = Ngalia, 61 = Nongra, 62 = Northampton, 63 = Northeast Tasmania, 64 = Officer, 65 = Ord, 66 = Paterson, 67 = Pedirka, 68 = Perth, 69 = Pilbara, 70 = Pine Creek, 71 = Polda, 72 = Proserpine, 73 = Quinkan, 74 = Rocky Cape, 75 = Savory, 76 = South Nicholson, 77 = Saint Vincent, 78 = Stuart, 79 = Styx, 80 = Surat, 81 = Sylvania, 82 = Tanami, 83 = Tennant Creek, 84 = Torrens, 85 = Torres Strait, 86 = Tyennan, 87 = Victoria River, 88 = Winnecke, 89 = Wiso, 90 = Yilgarn.

waterways termed paleochannels (Anand and Paine, 2002) or inset valleys (de Broekert and Sandiford, 2005) within the fossil system of much broader primary rivers. With the onset of semi-arid to arid climatic conditions in the Miocene this system of paleochannels has become segregated and clogged with sediments. Paleochannels are often marked by chains of salt lakes, and most have no surface flow

except after periods of exceptional rainfall (Anand and Paine, 2002). Calcrete accumulations have been deposited within these channels since the Pliocene, and commonly broaden into wide platforms and chemical deltas where entering major playas (McKay and Miezitis, 2001; Butt and Gray, 2007).

The announcement in 1972 by WMC Resources Ltd of the discovery of Yeelirrie (52,500 t U_3O_8 at 0.15% U_3O_8) sparked a flurry of exploration activity that resulted in the discovery of more than 60 additional calcrete-hosted uranium deposits and occurrences, including Lake Way-Centipede (10,835 t U_3O_8 at 0.04% U_3O_8), Lake Maitland (5,016 t U_3O_8 at 0.07% U_3O_8) and Thatcher Soak (4,100 t U_3O_8 at 0.03% U_3O_8) (McKay and Miezitis, 2001; Toro Energy Limited, 2008). The genetic model for the formation of calcrete-hosted uranium deposits in the Yilgarn Region is simple and well understood (Mann and Deutscher, 1978; Butt et al., 1984; McKay and Miezitis, 2001; Anand and Paine, 2002; Butt and Gray, 2007): Uranium and potassium are released by weathering of granitic rocks and transported laterally in the groundwater. Vanadium is derived either from exposed mafic to ultramafic basement rocks, or from the sediments underlying the calcrete. Both elements are being concentrated by focusing of

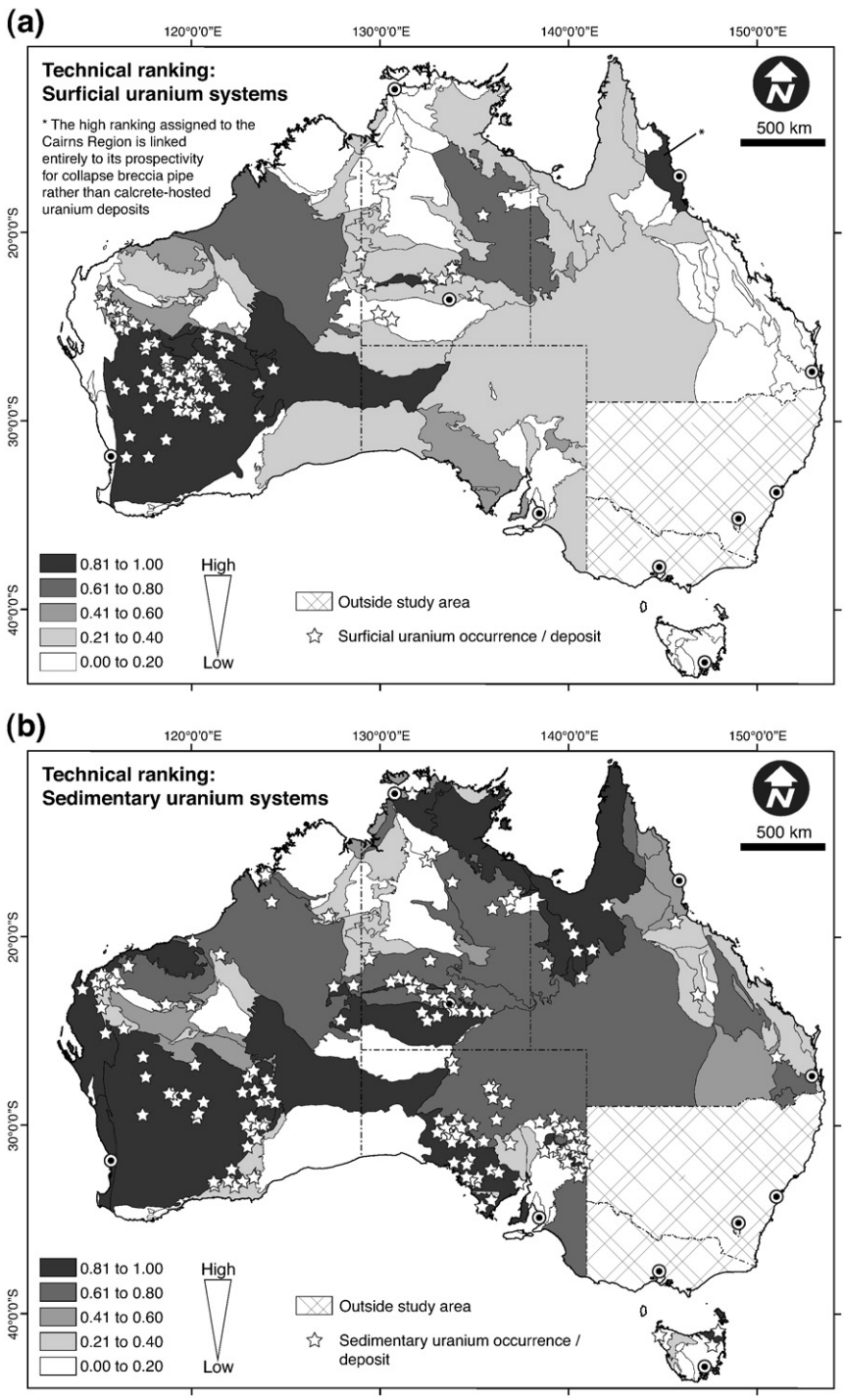

Fig. 5. Uranium prospectivity maps illustrating the technical ranking (i.e., probability of uranium mineralization) for (a) surficial, (b) sedimentary, (c) igneous-related, (d) metamorphic/metasomatic uranium systems, (e) unconformity-related, and (f) vein-related uranium systems. Probabilities were assigned according to the format presented in Tables 3a–3f and using Sherman–Kent scale in Table 4.

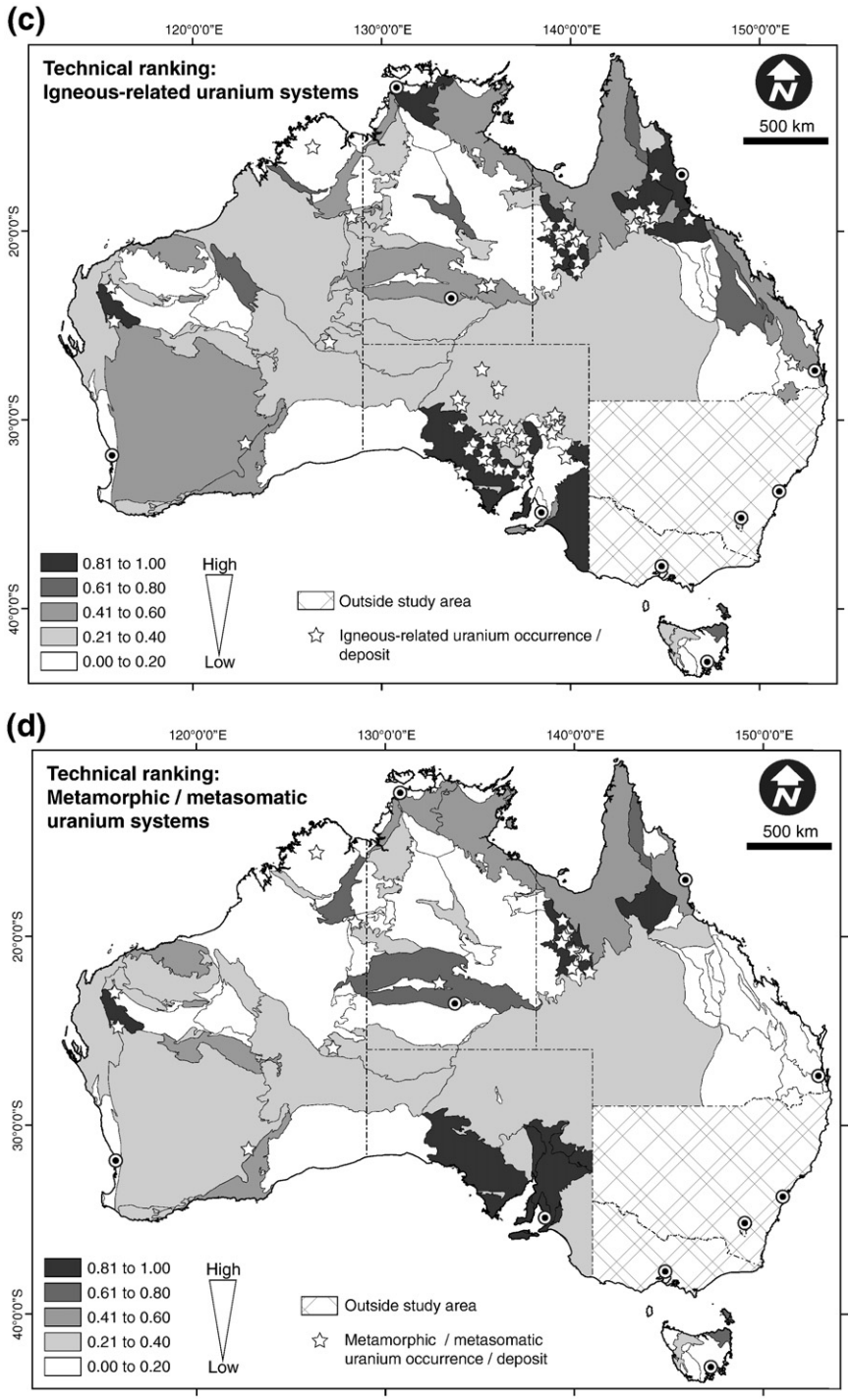

Fig. 5 (*continued*).

groundwaters and upward flow into calcrete aquifers. Precipitation of carnotite, the principal uranium mineral in calcrete-hosted uranium deposits, is triggered by chemical changes linked to upward percolation and evaporation of uranium-, vanadium- and potassium-bearing groundwaters.

Given the presence of all ingredients required to form calcrete-hosted uranium deposits and demonstrated endowment, the northeastern Yilgarn Region is highly prospective for surficial uranium systems and the surficial uranium systems model for this region scored probability values of 1.0 for all critical mineralization processes (Fig. 5a, Table 3a). We consider it very likely that future exploration will result in discovery of additional calcrete-hosted uranium deposits given the spatial and temporal coincidence of the identified critical mineralization processes over such a large geographic area. Even though the northeastern Yilgarn Region was subject to considerable uranium exploration activity and, therefore, is relatively mature for calcrete-hosted uranium deposits, one search space (cf. Hronsky and Groves, 2008) remains relatively under-explored: locations where calcrete accumulations and/or paleochannels are under cover. Deposits that may exist in such settings are blind with respect to gamma-ray spectrometric surveys that were instrumental in the discovery of most, if not all, surficial uranium

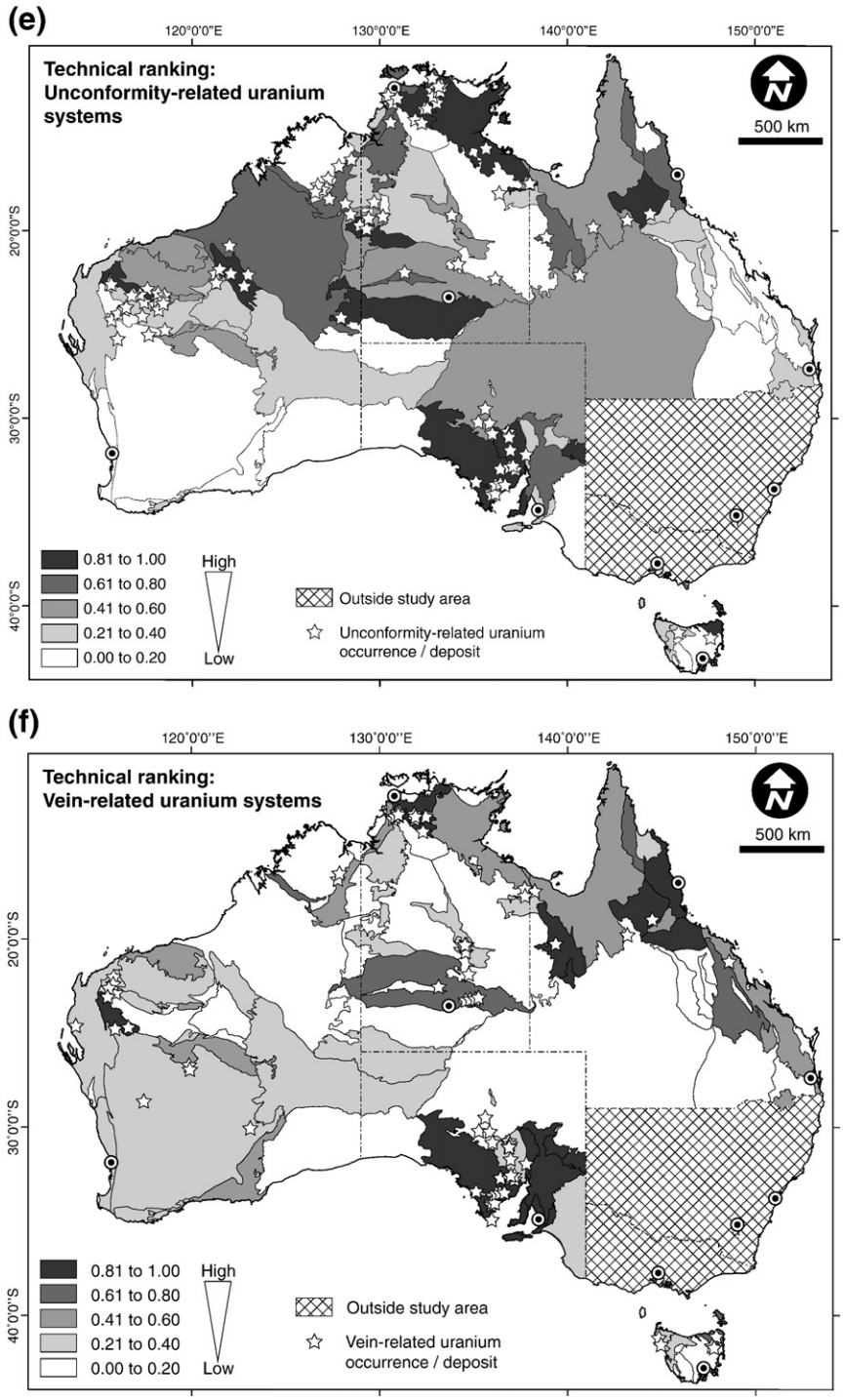

Fig. 5 (*continued*).

systems in the Yilgarn Region. The challenge for explorers is to identify the locations of buried channels and mineralized positions within them. Cases in point are the Old Station West and Downs East projects where Desert Energy Limited (2008) has identified previously unknown uraniferous calcretes in areas of widespread soils and sand cover.

At the time of this prospectivity analysis, the greenstone belts in the Yilgarn Region were almost completely under tenure, whereas most areas of granite and gneiss were only sparsely tenemented. In the most prospective northeastern Yilgarn Region, parcels of ground were available only over sections of paleodrainage and accumulations of valley calcrete away from the greenstone belts and, therefore, distal to potential sources of vanadium.

3.1.2. Musgrave Region (Northern Territory, South Australia, Western Australia)

The Musgrave Region (Fig. 4b) covers an area of 128,000 km^2. Its main geological element is the Musgrave Inlier, a Mesoproterozoic basement block bounded by cover rocks of the Neoproterozoic to Paleozoic Centralian Superbasin to the north (i.e., Amadeus Basin), south and west (i.e., Officer Basin), and Permian to Mesozoic Eromanga Basin to the east. The Paleo- to Mesoproterozoic basement

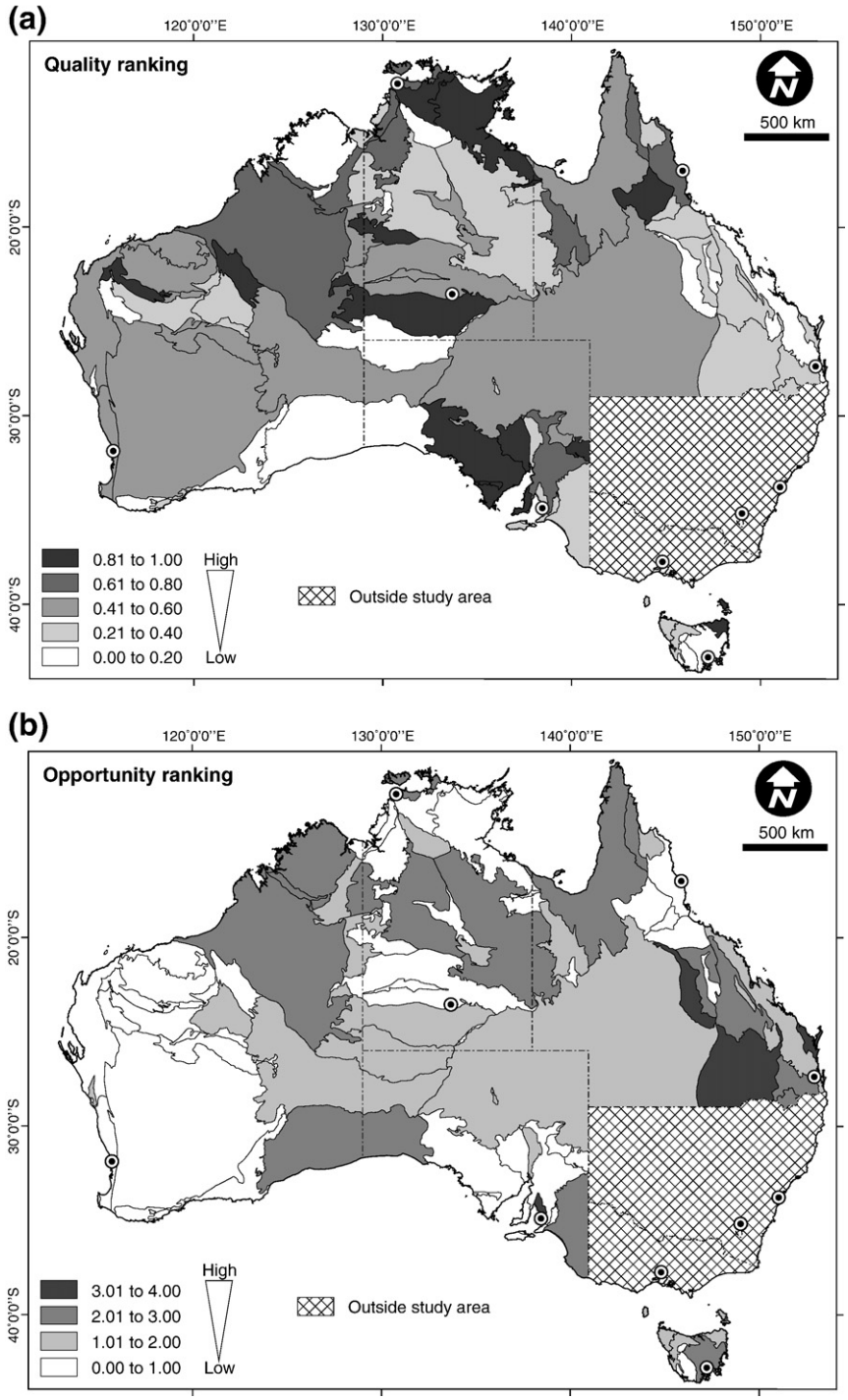

Fig. 6. Maps illustrating (a) quality ranking that highlights the geological regions with the greatest perceived potential for high-quality uranium systems characterized by high grades, large tonnages and/or relatively low mining costs (cf. Table 5), and (b) opportunity ranking that categorizes each geological region based solely on the amount of ground available for pegging and ranked on a scale from 1.0 (i.e., poor ground availability) to 4.0 (i.e., outstanding) (cf. Table 5).

of the Musgrave Inlier is made up of amphibolite- to granulite-grade quartzofeldspathic metamorphic rocks derived from igneous and minor sedimentary protoliths. These rocks were intruded by mafic to ultramafic and felsic rocks of various ages, and multiply deformed and metamorphosed between c. 1.6 Ga and 550 Ma. At c. 1.08 Ga the basement was intruded by mafic to ultramafic layered intrusions of the Giles Complex. The coeval Bentley Supergroup includes volcanic and minor sedimentary rocks of low-metamorphic grade and three large cauldron subsidence complexes of felsic volcanic rock and granite. The Musgrave region was exhumed from beneath the cover of the Centralian Superbasin during the c. 550 Ma Petermann Orogeny that was marked by north-directed thrusting, reactivation of shear zones and localised but pervasive greenschist–amphibolite facies metamorphism (Abeysinghe, 2003; Seat et al., 2007; Cawood and Korsch, 2008; Pirajno and Bagas, 2008). An extensive Cenozoic fossil river system with several 300 km-long drainage channels has been superimposed on the weathered land surface of the Musgrave Region. This paleodrainage system is marked by small playa lakes, alluvial sediments and calcrete accumulations that are exposed intermittently within the drainage.

Table 3a
Excerpt from prospectivity matrix: Yilgarn Region (Western Australia).

Uranium systems model	P_1 (Source)	P_2 (Transport)	P_3 (Deposition)	$P_{Mineralization}$ ($= P_1 \times P_2 \times P_3$)	Brief rationale for assignment of P_1 to P_3	Quality factor Q (see Table 5)	Quality ranking ($= P_{Mineralization} \times Q$)
Surficial (case study discussed in text)	1.00	1.00	1.00	1.00	P1: U source = U-rich Archean basement (granites); sources of V and K (greenstone belts; granites) P2: Transport media = extensive network of paleochannels and playa lakes P3: Appropriate climate = arid (paleo-) climatic conditions and high evaporation rates (in particular in the northeastern Yilgarn Region); Evidence for U mineralizing processes = numerous surficial (calcrete type) uranium deposits and occurrences	3.00	3.00
Sedimentary	1.00	1.00	1.00	1.00	P1: U Source = U-rich basement rocks, in particular granites (up to 130 ppm U) P2: Transport media = extensive network of paleochannels (up to 20 m deep); groundwaters; Archean pebble conglomerate occurrences P3: Geochemical evidence = reduced strata and lignite common in paleochannels in the southern Yilgarn Region; Evidence for U mineralizing processes: no known sedimentary U deposits but anomalous U and minor U occurrences recorded in paleochannels in the southern Yilgarn Region	5.00	5.00
Igneous-related	1.00	1.00	0.50	0.50	P1: Source = uranium-rich granites (up to 130 ppm) P2: Transport media = crustal breaks, shear zones and faults P3: Geochemical evidence = little data in the public domain that would help to better evaluate the potential of U-enriched granites (e.g., fractionation state, occurrence of pegmatite and/or igneous breccia); Evidence for U mineralizing processes: no known igneous-related U occurrences	2.00	1.00
Metamorphic/metasomatic	0.80	1.00	0.50	0.40	P1: Source = metamorphic basement rocks locally U enriched; fluids released during intrusive and metamorphic events P2: Transport media = crustal breaks, shear zones and faults P3: Geochemical evidence = little data in the public domain that would help to better evaluate the potential of the metamorphic basement, mapped redox boundaries; Evidence for U mineralizing processes: no known metamorphic/metasomatic U occurrences	1.00	0.40
Unconformity-related	1.00	0.40	0.50	0.20	P1: Source = uranium-rich basement rocks; P2: Transport media = no substantial intracratonic basins but minor basins are present (e.g., Permian Collie Basin, a graben-related, coaliferous basin); P3: Geochemical evidence = little data in the public domain that would help to better evaluate the potential of unconformities at the base of the minor basins; Evidence for U mineralizing processes: no known unconformity-related U occurrences	10.00	2.00
Vein-related	0.80	1.00	0.50	0.40	P1: Source = Metamorphic basement rocks locally U enriched; fluids released during intrusive and metamorphic events; P2: Transport media = crustal breaks, shear zones and faults; P3: Geochemical evidence = little data in the public domain that would help to better evaluate the potential of the metamorphic basement, mapped redox boundaries; Evidence for U mineralizing processes: No known metamorphic/metasomatic U occurrences	0.10	0.04
Opportunity ranking	Region is heavily tenemented but small parcels of ground are available over prospective paleodrainage in areas of granite						1.00
Overall ranking and comments	High potential for discovery of additional calcrete-hosted uranium deposits of small to large tonnage and low-grade, in particular within areas where prospective paleodrainage is under cover High potential for discovery of sedimentary uranium systems, in particular sandstone-hosted uranium deposits of low- to medium-grade and small to medium tonnage						5.00

Table 3b
Excerpt from prospectivity matrix: Musgrave Region (Western Australia, Northern Territory, South Australia).

Uranium systems model	P_1 (Source)	P_2 (Transport)	P_3 (Deposition)	$P_{Mineralization}$ ($=P_1 \times P_2 \times P_3$)	Brief rationale for assignment of P_1 to P_3	Quality factor Q (see Table 5)	Quality ranking ($= P_{Mineralization} \times Q$)
Surficial (case study discussed in text)	0.60	0.60	0.60	0.22	P_1: U source = Proterozoic granites, granulites and gneisses are locally U enriched; V source: Proterozoic mafic to ultramafic rocks, sediments in palaeochannels; K source = Proterozoic granites; note of caution = spatial coincidence of these sources documented for small portions of the Musgrave Region only P_2: Transport media = groundwaters, very low mean annual rainfall possibly translates into little water having been available for transporting U; Pathways = paleochannels, known calcrete accumulations but type and nature are unknown P_3: Appropriate climate = Musgrave Region has an arid climate and high evaporation rates; Evidence for U mineralizing processes = No known calcrete-hosted U occurrences	3.00	0.65
Sedimentary	0.60	0.70	0.40	0.17	P_1: U source = Proterozoic granites, granulites and gneisses are locally U enriched P_2: Transport media = groundwaters, very low mean annual rainfall possibly translates into little water having been available for transporting U; Pathways = paleochannels are present but it is not clear whether these are only shallow or more substantial drainage channels P_3: Geochemical evidence = no information regarding the presence of redox boundaries in paleochannels; Evidence for U mineralizing processes = No known sedimentary U occurrences	5.00	0.84
Igneous-related	0.60	0.75	0.50	0.23	P_1: U source = Proterozoic granites, granulites and gneisses are locally U enriched suggesting that favourable source conditions may have existed; P_2: Pathways = crustal breaks, faults; Transport media = hydrothermal fluids or highly fractionated granitic melts but there is little information in the public domain to support either model; P_3: Geochemical evidence = little information regarding the degree of fractionation of the granites and occurrence of pegmatites and igneous breccia; Evidence for U mineralizing processes = No known	2.00	0.45
Metamorphic/metasomatic	0.60	0.75	0.50	0.23	P_1: U source = Proterozoic granulites and gneisses are locally U enriched suggesting that favourable source conditions may have existed P_2: Transport media = magmatic or metamorphic fluids that interacted with the crystalline basement during Proterozoic episodes of deformation, magmatism and metamorphism; Pathways = crustal breaks, faults P_3: Geochemical evidence = little information about redox boundaries; Evidence for U mineralizing processes = No known metamorphic/metasomatic U occurrences	1.00	0.23
Unconformity-related	0.60	0.20	0.50	0.06	P_1: U source = Proterozoic granites, granulites and gneisses are locally U enriched P_2: Pathways = no substantial unconformity or intracratonic basin with permeable strata, although there is a very remote chance that such basins existed but are now eroded; Transport media: no information P_3: Geochemical evidence = little information about redox boundaries; Evidence for U mineralizing processes = no known unconformity-related U occurrences	10.00	0.60
Vein-related	0.60	0.75	0.50	0.23	P_1: U source = Proterozoic granulites and gneisses are locally U enriched suggesting that favourable source conditions may have existed P_2: Transport media = magmatic or metamorphic fluids that interacted with the crystalline basement during Proterozoic episodes of deformation, magmatism and metamorphism; Pathways = Crustal breaks, faults P_3: Geochemical evidence = little information about redox boundaries; Evidence for U mineralizing processes = no known metamorphic/metasomatic U occurrences	0.10	0.02
Opportunity ranking	2.00	Region is heavily tenemented in Western Australia but ground availablity is reasonable in South Australia and the Northern Territory; Large parcels of ground are available that are prospective for calcrete-hosted uranium deposits					
Overall ranking	0.84	Moderate probability of discovery of calcrete-hosted uranium deposits, most likely of low-grade and small to moderate tonnage; Moderate probability of discovery of igneous-related and metamorphic/metasomatic uranium deposits, grade-tonnage potential is highly speculative					

Table 3c
Excerpt from prospectivity matrix: Eromanga Region (South Australia).

Uranium systems model	P_1 (Source)	P_2 (Transport)	P_3 (Deposition)	$P_{Mineralization}$ ($=P_1 \times P_2 \times P_3$)	Brief rationale for assignment of P_1 to P_3	Quality factor Q (see Table 5)	Quality ranking ($=P_{Mineralization} \times Q$)
Surficial	1.00	1.00	0.50	0.50	P_1: U source = U-rich Proterozoic basement and hinterland (e.g., Curnamona Province, Arunta Inlier, Mount Isa Inlier), sediments derived from U-rich basement rocks; V source: No demonstrated sources; K source = Proterozoic basement and hinterland P_2: Transport media = meteoric waters, groundwaters; Pathways = paleochannels, known calcrete occurrences but type and nature are unknown, playa lakes P_3: Appropriate climate = semi-arid to arid climate with moderately high evaporation rates; Evidence for U mineralizing processes = no known calcrete-hosted U deposits and occurrences	3.00	1.50
Sedimentary (case study discussed in text)	1.00	1.00	1.00	1.00	P_1: U source = U-rich Proterozoic basement and hinterland (e.g., Curnamona Province, Arunta Inlier, Mount Isa Inlier), sediments derived from U-rich basement rocks P_2: Transport media = meteoric waters, groundwaters; Pathways = paleochannels, faults and fractures, permeable strata P_3: Geochemical evidence = mapped redox boundaries, known hydrocarbon occurrences; Evidence for U mineralizing processes = known sandstone-hosted U occurrences and significant deposits (e.g. Beverley, Four Mile, Honeymoon)	5.00	5.00
Igneous-related	0.02	0.90	0.20	0.00	P_1: U source = virtually no igneous rocks except for a few occurrences in an area that laps onto the Adelaide fold belt that is largely assigned to the adjacent Adelaide Region P_2: Pathways = crustal breaks, faults; transport media = hydrothermal fluids or highly fractionated granitic melts but there is little information to support either model P_3: Geochemical evidence = little information regarding the degree of fractionation of the local granites and occurrence of pegmatite or igneous breccia; Evidence for U mineralizing processes = some bedrock hosted U and Cu occurrences of unknown type	2.00	0.01
Metamorphic/metasomatic	0.90	0.90	1.00	0.81	P_1: U source = U content of locally exposed metamorphic basement rocks ranges from 10 to 15 ppm P_2: Transport media = magmatic or metamorphic fluids that interacted with the crystalline basement during Proterozoic or Palaeozoic episodes of deformation, magmatism and metamorphism; Pathways = crustal breaks and faults P_3: Geochemical evidence = little information about the presence of suitable redox boundaries; Evidence for U mineralizing processes = known U occurrences in similar metamorphic rocks in the adjacent Adelaide Region indicate some potential	1.00	0.81
Unconformity-related	0.50	0.90	0.75	0.34	P_1: U source = U content of locally exposed crystalline basement ranges from 10 to 15 ppm, intrabasinal sedimentary sequences likely to contain sufficient U P_2: Pathways = substantial unconformities present at base of the intracratonic Eromanga Basin; transport media: intrabasinal fluids P_3: Geochemical evidence = no information regarding the possible existence of a redox boundary between basin and basement; Evidence for U mineralizing processes = no known unconformity-related U occurrences	10.00	3.38
Vein-related	0.90	0.90	1.00	0.81	P_1: U source = U content of locally exposed metamorphic basement rocks ranges from 10 to 15 ppm P_2: Transport media = magmatic or metamorphic fluids that interacted with the crystalline basement during Proterozoic or Palaeozoic episodes of deformation, magmatism and metamorphism; Pathways = crustal breaks and faults P_3: Geochemical evidence = little information about the presence of suitable redox boundaries; Evidence for U mineralizing processes = known U occurrences in similar metamorphic rocks in the adjacent Adelaide Region indicate some potential	0.10	0.08
Opportunity ranking	1.00	Region is heavily tenemented, in particular the southwestern part that is highly prospective for sandstone-hosted U deposits and contains most of the known U endowment; Large parcels of ground are avilable some 100 to 200 km away from the inferred U source regions; Small parcels of ground are available that are prospective for vein-hosted uranium deposits in the crystalline basement					
Overall ranking and comments	5.00	High probability of discovery of additional sandstone-hosted U deposits, most likely of low- to medium-grade and small to large tonnage; Relatively high probability of discovery of metamorphic and vein-related U deposits in crystalline basement rocks, most likely of low-grade and small tonnage					

Table 3d
Excerpt from prospectivity matrix: Carnarvon Region (Western Australia).

Uranium systems model	P_1 (Source)	P_2 (Transport)	P_3 (Deposition)	$P_{Mineralization}$ ($=P_1 \times P_2 \times P_3$)	Brief rationale for assignment of P_1 to P_3	Quality factor Q (see Table 5)	Quality ranking ($=P_{Mineralization} \times Q$)
Surficial	1.00	0.40	0.40	0.16	P1: U source = U-rich hinterland (Yilgarn and Gascoyne regions); V source = no obvious source rocks; K source = Granites of the Yilgarn region P2: Transport media = groundwaters; Pathways = paleochannels, no valley calcrete or playa lake occurrences; terrace calcrete present in places; flow direction of drainage systems is towards the sea rather than inland; erosional rather than accumulation regime P3: Appropriate climate = evaporation rates are lower than those in the adjacent Yilgarn Region; Evidence for U mineralizing processes = numerous terrace-calcrete U occurrences immediately east	3.00	0.48
Sedimentary (case study discussed in text)	1.00	1.00	1.00	1.00	P1: U source = U-rich hinterland (Yilgarn and Gascoyne regions) P2: Transport media = groundwaters; Pathways = paleochannels, permeable strata, faults P3: Geochemical evidence = reduced strata, known redox boundaries, hydrocarbon occurrences; Evidence for U mineralizing processes = known sandstone-hosted U occurrences and deposits (e.g., Manyingee)	5.00	5.00
Igneous-related	0.50	1.00	0.50	0.25	P1: U source = virtually no igneous rocks except for those in an exposed Archean basement complex, the U content of these rocks is not known P2: Pathways = crustal breaks, faults; Transport media = hydrothermal fluids or highly fractionated granitic melts but there is li'le information to support either model P3: Geochemical evidence = no information regarding the degree of fractionation of granites and occurrence of pegmatite or igneous breccia in the exposed basement complex; Evidence for U mineralizing processes = no known igneous-related U occurrences	2.00	0.50
Metamorphic/metasomatic	0.50	1.00	0.50	0.25	P1: U source = virtually no metamorphic rocks except for those in an exposed Archean basement complex, the U content of these rocks is not known P2: Transport media = metamorphic fluids that were released during Archean episodes of deformation, magmatism and metamorphism; Pathways = crustal breaks and faults P3: Geochemical evidence = little information about the presence of suitable redox boundaries; Evidence for U mineralizing processes = no known metamorphic/metasomatic U occurrences	1.00	0.25
Unconformity-related	0.75	0.75	0.50	0.28	P1: U source = intrabasinal sedimentary sequences derived from U-rich source rocks but there is no information to support this option, U content of exposed Archean rocks is unknown P2: Pathways = unconformity at base of the intracratonic Carnarvon Basin, permeable strata, faults; transport media: intrabasinal fluids P3: Geochemical evidence = no information exists that would help to evaluate the redox potential at or immediately above/below the basal unconformity; Evidence for U mineralizing processes = no known unconformity-related U occurrences	10.00	2.81
Vein-related	0.50	1.00	0.50	0.25	P1: U source = virtually no metamorphic rocks except for those in an exposed Archean basement complex, the U content of these rocks is not known P2: Transport media = metamorphic fluids that were released during Archean episodes of deformation, magmatism and metamorphism; Pathways = crustal breaks and faults P3: Geochemical evidence = Little information about the presence of suitable redox boundaries; Evidence for U mineralizing processes = no known metamorphic/metasomatic U occurrences	0.10	0.03
Opportunity ranking	Region is heavily tenemented but good-sized parcels of ground are available over paleochannels that are considered prospective for sandstone-hosted U deposits						1.00
Overall ranking and comments	High probability of discovery of additional sandstone-hosted U deposits, most likely of low- to medium-grade and small to medium tonnage; High probability of discovery of calcrete-hosted U deposits but only of the low-grade and small tonnage (i.e., most likely uneconomic) terrace-type						5.00

Table 3e
Excerpt from prospectivity matrix: Pine Creek Region (Northern Territory).

Uranium systems model	P_1 (Source)	P_2 (Transport)	P_3 (Deposition)	$P_{Mineralization}$ ($=P_1 \times P_2 \times P_3$)	Brief rationale for assignment of P_1 to P_3	Quality factor Q (see Table 5)	Quality ranking ($=P_{Mineralization} \times Q$)
Surficial	1.00	0.40	0.40	0.16	P_1: U source = Archean and Proterozoic crystalline basement generally U enriched; V source: no demonstrated sources; K source = Archaean and Proterozoic crystalline basement rocks P_2: Transport media = meteoric waters and groundwaters; Pathways = extent and nature of paleodrainages poorly constrained, scarce and scaXered calcrete accumulations are present in the southern portion of the Pine Creek Region, no playa lakes P_3: Appropriate climate = no appropriate arid climatic conditions in the northern part of the Pine Creek Region; Evidence for U mineralizing processes = no known calcrete-hosted U occurrences	3.00	0.48
Sedimentary	1.00	0.90	0.90	0.81	P_1: U source = Archean and Proterozoic crystalline basement rocks, Proterozoic and younger sediments derived from U-rich basement rocks P_2: Transport media = Meteoric waters and groundwaters; Pathways = crustal breaks, faults, fractures, folds, unconformities and permeable strata, extent and nature of paleodrainages poorly known P_3: Geochemical evidence = Mapped redox boundaries are present at or near various Proterozoic unconformity surfaces, liXle is known about the redox potential of the Paleozoic and younger strata; Evidence for U mineralizing processes = no known sandstone-hosted U occurrences but excellent potential exists for structurally controlled, sandstone-hosted U deposits in Proterozoic sandstones and conglomerates of the McArthur Basin, Cambrian and undivided Cretaceous sandstones and pebble conglomerate of the Dunmarra Basin	5.00	4.05
Igneous-related	1.00	1.00	0.90	0.90	P_1: U source = U-rich Archean and Proterozoic crystalline basement (in particular granites), fluids released during Archean and Proterozoic igneous events P_2: Pathways = crustal breaks, shear zones, faults and Archean to Paleoproterozoic unconformities; Transport media = hydrothermal fluids or highly fractionated granitic melts P_3: Geochemical evidence = fertile fractionated granite suites (e.g., Cullen Supersuite, Allia Creek Suite, Jim Jim Suite) with potential for and/or known Cu, Sn and Au mineralization; Evidence for U mineralizing processes = known granite-hosted uranium occurrences in the Cullen Batholith	2.00	1.80
Metamorphic/metasomatic	0.75	1.00	1.00	0.75	P_1: U source = U-rich Archean and Proterozoic crystalline basement (in particular granites), fluids released during Archean and Proterozoic igneous and metamorphic events P_2: Transport media = magmatic, metamorphic or hydrothermal fluids that interacted with the crystalline basement during Proterozoic episodes of deformation, magmatism and metamorphism; Pathways = crustal breaks, faults, unconformities P_3: Geochemical evidence = known redox boundaries at or close to mapped unconformity surfaces; Evidence for U mineralizing processes = no known metamorphic/metasomatic U occurrences, although some of the known vein-type U deposits could fall within this category	1.00	0.75
Unconformity-related (case study discussed in text)	1.00	1.00	1.00	1.00	P_1: U source = crystalline Archean and Proterozoic basement is commonly U-rich, intrabasinal sedimentary sequences derived from U-rich basement rocks may have provided additional U P_2: Pathways = unconformities, crustal breaks, faults; Transport media = intrabasinal fluids, basement (metamorphic/hydrothermal) fluids P_3: Geochemical evidence = known redox boundaries between basin and basement; Evidence for U mineralizing processes = known unconformity-related uranium occurrences and substantial deposits (e.g., Ranger, Yabiluka)	10.00	10.00
Vein-related	1.00	1.00	0.90	0.90	P_1: U source = U-rich Archean and Proterozoic crystalline basement (in particular granites), fluids released during Archean and Proterozoic igneous and metamorphic events P_2: Transport media = magmatic, metamorphic or hydrothermal fluids that interacted with the crystalline basement during Proterozoic episodes of deformation, magmatism and metamorphism; Pathways = crustal breaks, faults, unconformities P_3: Geochemical evidence = known redox boundaries at or close to mapped unconformity surfaces, reduced strata common in the Rum Jungle area; Evidence for U mineralizing processes = known vein-type U occurrences and deposits (e.g., ABC, Adelaide River, Fleur de Lys)	0.10	0.09
Opportunity ranking	1.00	Region is extremely heavily tenemented Small parcels of ground are available that are prospective for unconformity-related uranium deposits but these are fragmented and fraught with issues (e.g., too many underlying landholders, located next to nature reserves, national parks or water reservoirs)					
Overall ranking and comments	10.00	High probability of discovery of additional unconformity-related uranium deposits, in particular in areas of shallow cover and most likely of medium- to high-grade and small to medium tonnage Relatively high potential for discovery of structurally controlled sandstone-hosted uranium deposits, most likely of low to medium-grade and small to medium tonnage					

Table 3f
Excerpt from prospectivity matrix: King Leopold Region (Western Australia).

Uranium systems model	P_1 (Source)	P_2 (Transport)	P_3 (Deposition)	$P_{Mineralization}$ ($=P_1 \times P_2 \times P_3$)	Brief rationale for assignment of P_1 to P_3	Quality factor Q (see Table 5)	Quality ranking ($=P_{Mineralization} \times Q$)
Surficial	1.00	0.20	0.90	0.18	P_1: U source = U-rich Proterozoic basement, in particular felsic volcanic rocks and granites (background values >10 ppm U); V source: Proterozoic basement rocks are locally V-rich; K source = Proterozoic felsic volcanic rocks and granites P_2: Transport media = meteoric waters, groundwaters; Pathways = Early Devonian to early Permian paleochannels that drain into the Canning Region, no known calcretes, no playa lakes P_3: Appropriate climate = region has a semi-arid climate with high evaporation rates but a much higher mean annual rain fall than the Yilgarn Region, the type location for calcrete-hosted U deposits; Evidence for U mineralizing processes = no known calcrete-hosted U occurrences	3.00	0.54
Sedimentary	1.00	0.90	0.75	0.68	P_1: U source = U-rich Proterozoic basement, in particular felsic volcanic rocks and granites (background values >10 ppm U) P_2: Transport media = meteoric waters, groundwaters; Pathways = Early Devonian to early Permian palaeochannels that drain into the Canning Region, permeable strata, faults P_3: Geochemical evidence = no information regarding redox boundaries within palaeochannels; Evidence for U mineralizing processes = no known sandstone-hosted U occurrences and deposits but U deposits are present in palaeochannels in the adjacent Canning Region and these channels have the same source region	5.00	3.38
Igneous-related	1.00	1.00	0.75	0.75	P_1: U source = Proterozoic granites and volcanic rocks P_2: Pathways = crustal breaks, faults; Transport media = magmatic or hydrothermal fluids, or highly fractionated granitic melts P_3: Geochemical evidence = fractionated granites and pegmatites; Evidence for U mineralizing processes = the adjacent Halls Creek Region contains numerous U occurrences that are hosted by the Whitewater Volcanics, a geological unit that is also present in the King Leopold Region	2.00	1.50
Metamorphic/metasomatic	0.40	1.00	0.75	0.30	P_1: U source = limited amount of metamorphic rocks and these commonly have low U content, contact metamorphism/metasomatism only affected very small rock volumes P_2: Transport media = magmatic or metamorphic fluids that interacted with the crystalline basement during Proterozoic episodes of deformation, magmatism and metamorphism; Pathways = crustal breaks and faults P_3: Geochemical evidence = little information regarding the presence of suitable redox boundaries; Evidence for U mineralizing processes = no known metamorphic/metasomatic U occurrences	1.00	0.30
Unconformity-related (case study discussed in text)	1.00	1.00	0.75	0.75	P_1: U-rich Proterozoic basement, in particular felsic volcanic rocks and granites (background values >10 ppm U); P_2: Pathways = substantial unconformity that seperates Palaeoproterozoic basement rocks of the Hooper Complex from Paleoproterozoic sedimentary rocks and minor felsic volcanic rocks of the Speewah Basin; Transport media: Intrabasinal fluids; P_3: Geochemical evidence = it is likely that significant redox gradients exist between basin and basement; Evidence for U mineralizing processes = no known unconformity-related U occurrences but such occurrences are present in the adjacent Halls Creek Region and in a geological environment that is also present in the King Leopold Region	10.00	7.50
Vein-related	1.00	1.00	0.75	0.75	P_1: U source = limited amount of metamorphic rocks and these commonly have low U contents P_2: Transport media = magmatic or metamorphic fluids that interacted with the crystalline basement during Proterozoic episodes of deformation, magmatism and metamorphism; Pathways = crustal breaks, faults P_3: Geochemical evidence = little information regarding the presence of suitable redox boundaries; Evidence for U mineralizing processes = potential vein-hosted U occurrences (e.g., Juno and Jupiter)	0.10	0.08
Opportunity ranking	3.00	Region is heavily tenemented Substantial parcels of ground are available that are prospective for unconformity-related and igneous-related U deposits					
Overall ranking and comments	7.50	Relatively high probability of discovery of unconformity-related uranium deposits, most likely of medium- to high-grade and small to medium tonnage Moderate to relatively high probabilities of discovery of vein- and igneous-related U deposits, most likely of low- to medium-grade and small tonnage					

Table 4
Sherman–Kent scale for quantifying subjective probability estimates.
Modified from Jones and Hillis, 2003).

Numerical probability value	Subjective probability estimates
0.98–1.00	Proven; definitely true
0.90–0.98	Virtually certain; convinced
0.75–0.90	Highly probable; strongly believe; highly likely
0.60–0.75	Likely; probably true; about twice as likely to be true as untrue; chances are good
0.40–0.60	Chances are slightly better than even or slightly less than even
0.50–0.50	Chances are about even; it can be true or not
0.20–0.40	Could be true but more probably not; unlikely; chances are fairly poor; two or three times more likely to be untrue than true
0.02–0.20	Possible but very doubtful; only a slight chance; very unlikely indeed; very improbable
0.00–0.02	Proven untrue; impossible

There are no known calcrete-hosted uranium deposits in the Musgrave Region. In fact, our investigations indicate that this remote region has never been explored for surficial uranium systems. Hence, in contrast to the Yilgarn Region that has been explored for calcrete-hosted uranium deposits since the 1970s, the Musgrave Region is data-poor with respect to information that would help to assess its potential for surficial uranium systems. Given the lack of data and greater uncertainty, the probability values assigned to the critical mineralization processes (P_1 to P_3) of the surficial uranium systems model for the Musgrave Region (Fig. 5a, Table 3b) are consistently lower than those of the surficial uranium systems model for the Yilgarn Region. For example, there appears to be no information in the public domain about the type and morphology of calcrete accumulations in this region. However, given that many calcretes occur within or next to paleodrainage channels, it is likely that these accumulations are valley calcretes similar to those that host surficial uranium systems in the northeastern Yilgarn Region. In addition, little is known about the spatial distribution and quality of the likely sources of uranium and vanadium in the Musgrave Region. Publicly available gamma-ray spectrometric and OZCHEM whole rock geochemistry data indicate that at least some Proterozoic units are enriched in uranium with certain granites containing up to 49.5 ppm U. The inferred uranium source potential of some igneous suites in the Musgrave Region has been demonstrated by a new map of the uranium content of igneous rocks of Australia (Schofield, 2009a,b,c,d). The most likely sources of vanadium in the Musgrave Inlier are the many mafic to ultramafic rocks with some comprising vanadium- and titanium-bearing magnetite layers that contain more than 7,000 ppm V.

The Musgrave Region contains all ingredients required to form calcrete-hosted uranium deposits, including presence of extensive Tertiary paleodrainage systems, calcrete accumulations within and adjacent to drainage lines, appropriate sources of uranium, potassium and vanadium, and arid climatic conditions. However, the spatial and temporal coincidence of the essential ingredients is currently demonstrated for small areas within the Musgrave Region only. Moreover, there are no known uranium occurrences in the Musgrave Region and no significant radiometric anomalies over any of the exposed calcrete accumulations. As such, the technical ranking (i.e., $P_{Mineralization}$) of the Musgrave Region is relatively low. Nevertheless, conceptually this region looks very interesting and its ranking may be upgraded once more uranium specific data become available for this remote area.

At the time of this analysis, the Musgrave Region was heavily tenemented in Western Australia but large parcels of ground were available over several calcrete accumulations within and adjacent to paleodrainage lines. Ground availability was reasonable in those parts of the Musgrave Region that fall within the jurisdictions of South Australia and the Northern Territory.

3.2. Sedimentary uranium systems

3.2.1. Eromanga Region (New South Wales, Northern Territory, Queensland, South Australia)

The Eromanga Region (Fig. 4b) covers an area of 1,178,000 km^2. Despite its large size and remoteness, a wealth of geological data is available for this region because it has been explored by oil and gas companies since the 1950s (Cotton et al., 2006) and uranium companies since the late 1960s (McKay and Miezitis, 2001; Skirrow et al., 2009b), and is well endowed with respect to these natural resources (McKay and Miezitis, 2001; Cotton et al., 2006; Skirrow et al., 2009b).

The largest geological element of this region, the Mesozoic Eromanga Basin, is an intracratonic sag basin that overlies Precambrian basement and Neoproterozoic to late Paleozoic sedimentary basins and, in turn, is overlain by Cenozoic sedimentary basins. Stratigraphically, the Eromanga Basin is subdivided into three main phases: (1) Early Jurassic to Early Cretaceous non-marine successions (i.e., medium-grained sandstones that were deposited in a braided fluvial environment, followed by fine-grained sandstones, siltstones and shales that were deposited in a lacustrine environment); (2) Early Cretaceous marine successions (i.e., basal sandstones, followed by

Table 5
Rationale for quality ranking of the six newly proposed uranium systems models.

Uranium systems model	Quality factor (Q)	Rationale
Unconformity-related	10	Ore zones are commonly high-grade and tonnages generally range from medium to large Mining and metallurgical procedures are well-established In 2006, unconformity-related uranium deposits produced more than 33% of the world's uranium
Sedimentary	5	Ore zones are commonly low- to medium-grade and tonnages range from small to large Sandstone-hosted uranium deposits are the economically most attractive of the sediment-hosted uranium deposits, in particular when amenable to in-situ recovery (ISR) mining (e.g., Beverley uranium mine) In 2006 ISL mining operations produced 26% of the world's uranium
Surficial	3	Ore zones are commonly low-grade and tonnages range from small to large Occur close to surface and therefore relatively inexpensive to mine Carnotite, the main uranium mineral in calcrete-hosted uranium deposits, is amenable to an alkaline leaching process (e.g., Langer Heinrich uranium mine)
Igneous	2	Ore zones are commonly low- to medium-grade and tonnages range from small to large Mining and metallurgical procedures are well-established, in particular for intrusion-related uranium deposits
Metamorphic/metasomatic	1	Ore zones are commonly low-grade and tonnages are often small Potential recovery issues due to the refractory nature of certain ore assemblages (e.g., brannerite-rich ore at the Valhalla uranium deposit)
Vein	0.1	Ore zones are commonly low-grade and tonnage are mainly small Deposits are generally narrow and structurally complex and, therefore, can be difficult to mine

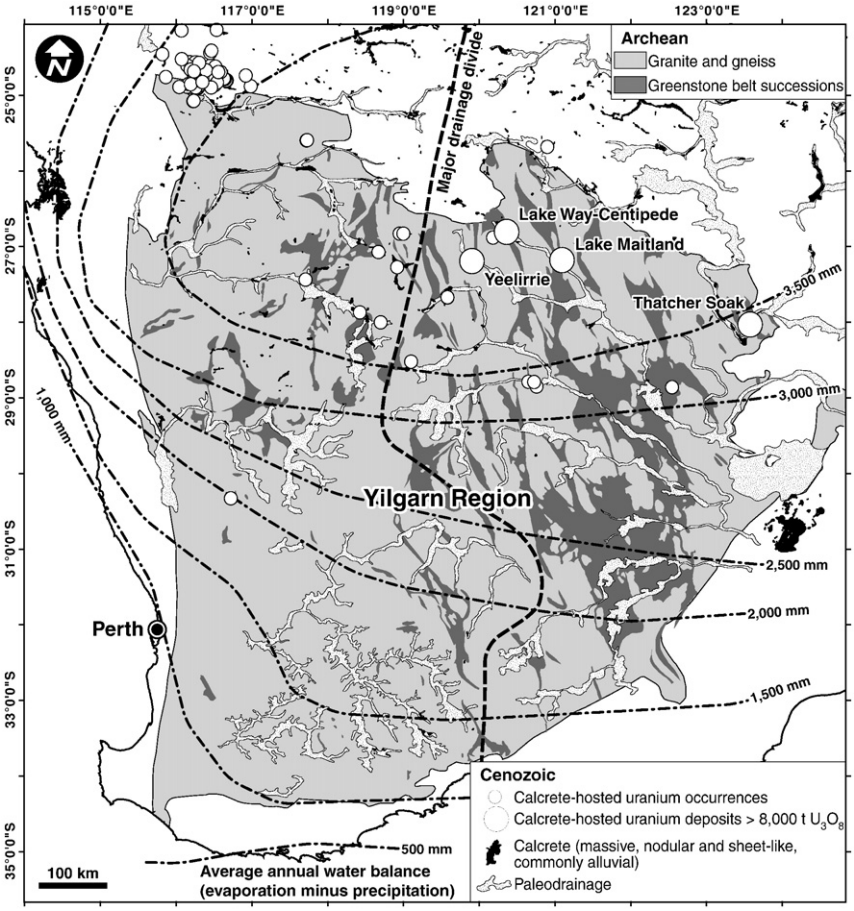

Fig. 7. Calcrete-hosted uranium deposits in the Yilgarn Region and adjacent geological regions in Western Australia. These deposits are spatially and genetically associated with an extensive paleodrainage system. Calcrete accumulations have formed within this system since the Pliocene (Anand and Paine, 2002; de Broekert and Sandiford, 2005). This overview map serves to illustrate part of the significant amount of information availble for what is the type locality of this particular style of uranium deposit. The area of greatest endowment and exploration potential in the northeastern Yilgarn Region is bounded by the major continental drainage divide to the east (i.e., partly linked to the greater potential for pooling and evaporation of groundwaters in east-draining channels), average water balance isoline of ±3,500 mm to the south and the boundary of exposed granite–gneiss and greenstone belts of the Archean Yilgarn Craton to the north and east (i.e., limit of supply of uranium, potassium and vanadium for forming the uranium mineral carnotite).

shales and mudstone that were deposited in a deeper water environment); and (3) Late Cretaceous non-marine successions (i.e., sandstone, shale and siltstone that were deposited in a low-energy fluvial to lacustrine environment). The combined thickness of these successions is up to 3 km (Drexel and Preiss, 1995; Cotton et al., 2006; Skirrow et al., 2009b). Organic matter is abundant in several units (e.g., Early Cretaceous Toolebuc Formation and Bulldog Shale). Coal seams are present in the lower and upper non-marine successions of the Eromanga Basin, and oil and gas have been recovered from almost all of the lower non-marine units in the Moomba region of the Eromanga Basin (Cotton et al., 2006; Skirrow et al., 2009b). There are no known uranium deposits in the Eromanga Basin but recent work by Skirrow et al. (2009b) suggests that if suitable reductants were available, sandstone-hosted uranium deposits could have formed in the Late Cretaceous or Paleocene aquifers. Most uranium companies (e.g., Uranium Equities Limited, 2008) that are currently exploring the Eromanga Basin target roll front-style uranium mineralization analogous to that in the Chu-Sarysu and Syrdarya uranium fields of Kazakhstan (Jaireth et al., 2008).

The Mesozoic Eromanga Basin is unconformably overlain by sedimentary successions of the Cenozoic Lake Eyre Basin, a product of tectonic subsidence and episodic fluvial and lacustrine sedimentation that commenced in the Late Paleocene and continues to the present day. Stratigraphically, the Lake Eyre Basin is subdivided into three main phases (Alley, 1998): (1) Late Paleocene to Middle Eocene fluvio-lacustrine successions (i.e., sand, silt, clay and carbonaceous horizons); (2) Late Oligocene to Miocene lacustrine successions (i.e., dolomite and magnesium-rich clay and sand); and (3) Pliocene and Quaternary fluvial, lacustrine and aeolian successions (i.e., red clay, silt and sand). The Birdsville Track Ridge divides the Lake Eyre Basin into two sub-basins, the Tirari Sub-basin in the northwest and Callabonna Sub-basin in the southeast. From a uranium perspective, the key units in the Lake Eyre Basin are the Eocene Eyre Formation, which occurs in the Tirari and Callabonna sub-basins, and Miocene Namba Formation, which occurs in the Callabonna Sub-basin only (Alley, 1998; Hou et al., 2007b; Skirrow et al., 2009b). The Eyre Formation comprises well-sorted pyritic and carbonaceous sands that were deposited by braided streams at the base of the Lake Eyre Basin. Most of the known, significant uranium deposits of the Lake Eyre Basin are in a paleodrainage system in the Lake Frome region of the Callabonna Sub-basin, filled by sands of the Eyre Formation. This paleodrainage system contains Four Mile (western zone: 15,000 t U_3O_8 at 0.37% U_3O_8; eastern zone: 14,400 t U_3O_8 at 0.31% U_3O_8), Honeymoon (2,900 t U_3O_8 at 0.24% U_3O_8), East Kalkaroo (4,000 t U_3O_8 at 0.18% U_3O_8) and Goulds Dam (17,600 t U_3O_8 at 0.12% U_3O_8) (McKay and Miezitis, 2001; Skirrow et al., 2009b). Preferred localities of uranium mineralization are channel bends and/or sites of confluence with tributaries. The general shape and orientation of the individual channels are controlled by basement rocks and structures (Jaireth et al., 2010). Uranium mineralization at the Beverley uranium mine (21,000 t U_3O_8 at 0.27% U_3O_8) is in the Namba Formation, which was deposited in a fluvial lacustrine environment with meandering

streams and billabongs and overlies the Eyre Formation disconformably. At Beverley, the Namba Formation is divided into the basal Alpha Mudstone, overlying Beverley Sands (aquifer) and uppermost Beverley Clay. Much of the uranium mineralization is located in sinuous depressions in the upper surface of the Alpha Mudstone that are filled by carbonaceous, pyritiferous sediments of the Beverley Sands (Skirrow et al., 2009b; Jaireth et al., 2010).

The fertility of the Eromanga Region is demonstrated by the occurrence of numerous significant roll front-style sandstone uranium deposits in the Lake Frome region of the Callabonna Sub-basin. Given certain analogies with the Chu-Sarysu and Syrdarya uranium fields of Kazakhstan (Jaireth et al., 2008), additional uranium potential may even exist in those parts of the Cenozoic Callabonna Sub-basin that are some 100 to 200 km away from suitable uranium source rocks. Significant uranium potential also exists in the Cretaceous Eromanga Basin, in particular within reduced strata near the boundary with uranium-rich rocks of the Gawler Craton, Curnamona Province, Arunta Inlier and Mount Isa Inlier. Given the known uranium endowment and presence of (1) extensive paleodrainage systems; (2) uranium-enriched basement rocks at the margins of (i.e., Gawler Craton, Curnamona Province, Arunta Inlier, Mount Isa Inlier) and underneath the basins of the Eromanga Region; (3) meteoric waters; (4) permeable strata interstratified with aquitards or aquicludes; and (5) mobile (e.g., gaseous or liquid hydrocarbons) and in-situ (e.g., organic matter or pyrite as in the Bulldog Shale, Toolebuc Formation, Eyre Formation and Namba Formation) reductants within aquifers or aquitards, the sedimentary uranium systems model for the Eromanga Region scored probability values of 1.0 for all critical mineralization processes (i.e., $P_{Mineralization}$ of 1.0) and relatively high quality ranking of 5.0 (Fig. 5b, Table 3c).

At the time of the manual prospectivity analysis, the margin of the Eromanga Region was heavily tenemented, in particular the highly prospective southwestern margin where most of the known uranium occurrences and deposits are concentrated. Large parcels of ground were available only further into the Eromanga and Lake Eyre basins and, consequently, further away from the known uranium source

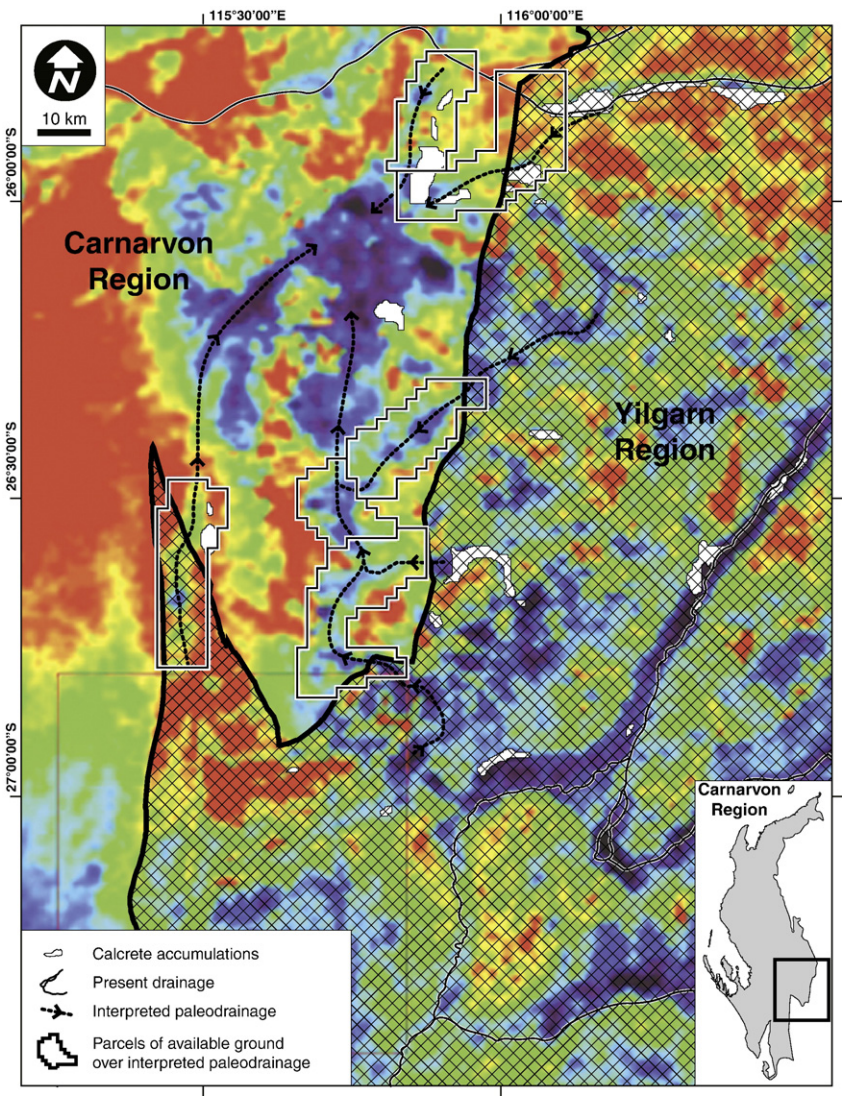

Fig. 8. National Oceanic and Atmospheric Administration — Advanced Very High Resolution Radiometer (NOAA-AVHRR) thermal imagery over parts of the southeastern Carnarvon and adjacent Yilgarn regions. This type of remote sensing data is useful for visualizing temperature variations (red colors = warmest; dark blue colors = coldest) in the subsurface. Given the elevated moisture content, (paleo-) drainage channels commonly coincide with areas of relatively cold subsurface temperatures. As such, thermal data can be used as a quick and inexpensive method for mapping palaeochannels, particularly when used in conjunction with other datasets (Hou et al., 2007a,b). This image shows several interpreted channels that do not coincide with the present day drainage. These inferred paleochannels emanate from mainly granitic, likely uranium-enriched source regions in the Yilgarn Region and are incised into sedimentary rocks of the late Carboniferous to late Permian Lyons Group and early Permian Wooramel Group of the Carnarvon Basin. Inset: Outline of the Carnarvon Region and box illustrating coverage of the NOAA-AVHRR image.

regions. However, these areas could be highly prospective if the Chu-Sarysu and Syrdarya uranium deposit model is applicable to the Eromanga Region.

3.2.2. Carnarvon Region (Western Australia)

The Carnarvon Region (Fig. 4b) covers an area of 122,000 km^2 and coincides with the onshore part of the greater Carnarvon Basin (see plates 1 to 3 in Hocking et al., 1987), an up to 12 km deep intracontinental rift basin of Paleozoic to Cenozoic age. The basin stratigraphy comprises: (1) Silurian continental to shallow-marine sedimentary rocks (mainly red sandstones, dolomite, shale and evaporitic sequences such as halite beds); (2) Devonian deltaic and shallow-marine sedimentary rocks (mainly sandstones and limestones); (3) Carboniferous shallow-marine carbonates, sandstones and conglomerates; (4) Permian glacial, fluvioglacial, and shallow-marine sedimentary rocks (mainly conglomerates, sandstones and limestones); and (5) Triassic to Tertiary marine and continental sedimentary rocks (mainly sandstone, siltstone, shale and limestone). Reduced to strongly reduced carbonaceous, pyritic, lignitic and coaliferous strata and unconformities are common. The Carnarvon Basin also contains hydrocarbon accumulations (Hocking et al., 1987), a factor that is relevant for assessing uranium prospectivity given a common spatial association of sandstone uranium deposits and hydrocarbon-bearing basins (Jaireth et al., 2008).

Uranium exploration in the Carnarvon Region in the 1970s and 1980s recorded significant amounts of uranium in groundwaters from Cretaceous and Cenozoic aquifers. Exploration also delineated several paleochannels that are incised into uranium-enriched Proterozoic granite basement and contain Cretaceous sediment fill. Follow-up work ultimately resulted in the discovery of the Manyingee (12,078 t U_3O_8 at 0.09% U_3O_8) and Bennetts Well (1,500 t U_3O_8 at 0.16% U_3O_8) sandstone-hosted rollfront-type uranium deposits (McKay and Miezitis, 2001).

The Carnarvon Region is considered highly prospective for sedimentary uranium systems of late Paleozoic to Mesozoic age (Fig. 5b, Table 3d). Given the presence of (1) demonstrated uranium sources (Archaean granites in the adjacent Yilgarn Region), (2) suitable pathways for transport of uranium from source to trap (known Paleozoic to Mesozoic paleochannels and permeable strata), (3) ingredients required for uranium deposition (known redox boundaries and uranium deposits within paleochannels of the Carnarvon Region), and (4) sedimentary uranium deposits, the

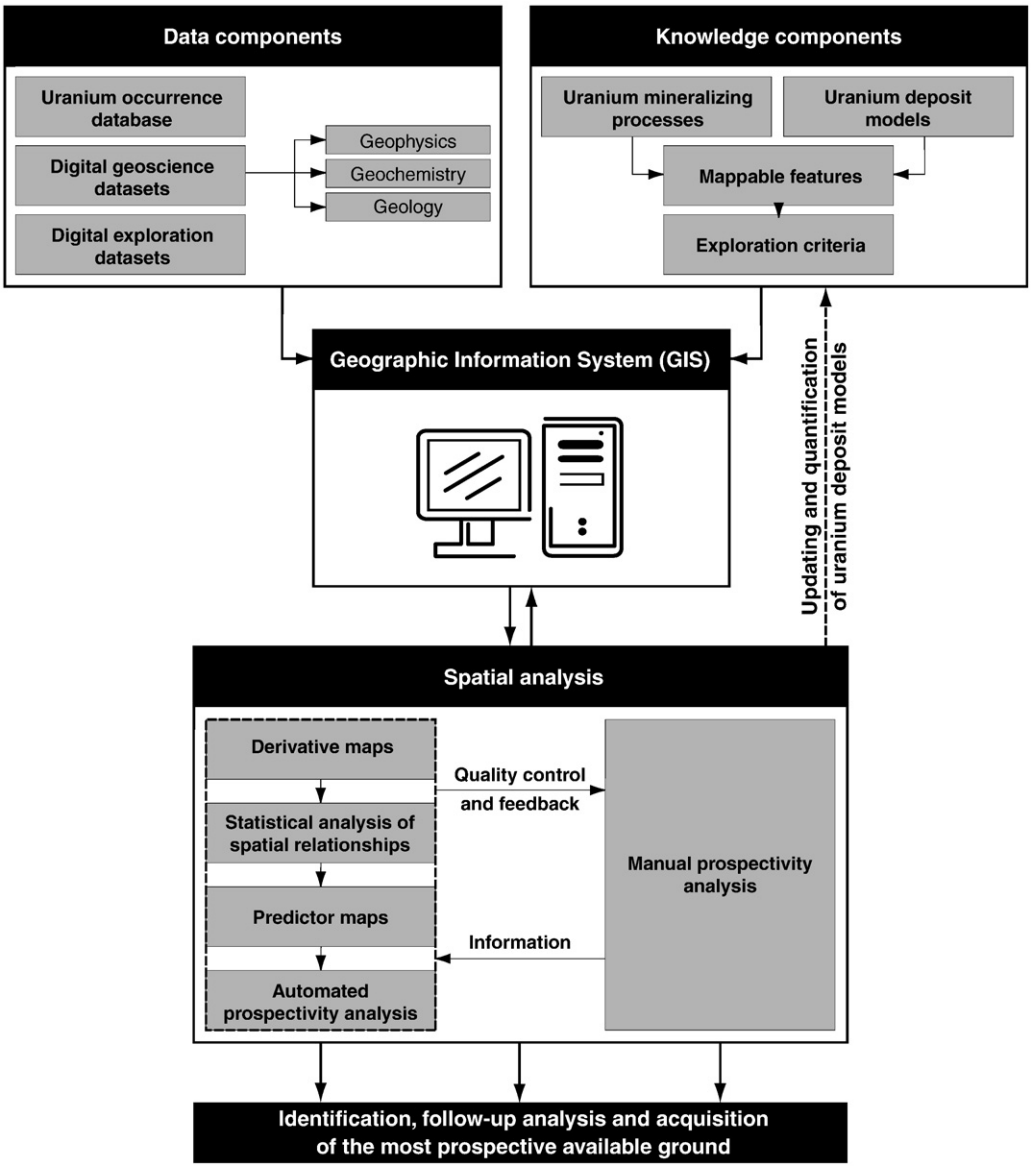

Fig. 9. Schematic representation of the approach taken in this continent-wide analysis of uranium potential, which combines manual GIS-assisted (this paper) and automated GIS-driven methods (the topic of a companion paper that will be submitted in early 2011).

sedimentary uranium systems model scored probability values of 1.0 for all critical mineralization processes. The geological framework and knowledge about known uranium occurrences suggest that the most likely uranium deposit types in the Carnarvon Region are rollfront and paleochannel-hosted ones with low to medium grades and small to medium tonnages.

National Oceanic and Atmospheric Administration — Advanced Very High Resolution Radiometer (NOAA-AVHRR) imagery (Fig. 8) (cf. Hou et al., 2007a) covering the southern Carnarvon Region helped to delineate several probable paleochannels under Cenozoic sediment cover that emanate from mainly granitic, likely uranium-enriched source regions in the Yilgarn Craton. The main flow directions of these inferred drainages are parallel to the principal structural trends in this area: NE–SW and N–S. According to surficial and interpretative bedrock geological maps by the Geological Survey of Western Australia, these channels are most likely incised into sedimentary rocks of the late Carboniferous to late Permian Lyons Group and early Permian Wooramel Group. If these inferred drainages (1) contain any reduced strata (e.g., carbonaceous, lignitic and pyritic sandstone, siltstone and shale as are common in the Permian, Jurassic and Cretaceous successions of the Carnarvon Region); (2) transect regional redox boundaries; and/or (3) intersect with pathways of hydrocarbons or H_2S released from underlying oil or gas occurrences, it is possible that economic concentrations of uranium accumulated in these channels.

At the time of the manual uranium prospectivity analysis, the Carnarvon Region was heavily tenemented and the level of opportunity that existed with respect to ground being available for pegging was low. Hence, the Carnarvon Region received a low opportunity ranking of one on a scale of one to four.

3.3. Unconformity-related uranium systems

3.3.1. Pine Creek Region (Northern Territory)

The Pine Creek Region (Fig. 4b) covers an area of 45,000 km^2, including the central Marrakai and eastern Nimuwah domains of the Pine Creek Orogen but excluding the Litchfield Domain that makes up the western part of the fold belt. The Pine Creek Orogen comprises a 14 km-thick sequence of variably deformed Paleoproterozoic metasedimentary, volcaniclastic and minor volcanic rocks that were deposited in an intracratonic rift basin. These rocks were intruded by pretectonic dolerite sills and unconformably overlie late Archaean basement that is exposed in dome structures (i.e., Rum Jungle and Nanambu complexes) that mainly comprise granite, gneiss and minor metasedimentary rocks. Regional deformation during the 1.86 to 1.84 Ga Barramundi Orogeny produced tight folds and penetrative structural fabrics. In the course of this event, rocks in the central Pine Creek Orogen were metamorphosed to lower greenschist facies, whilst metamorphic grades in the eastern and western parts reached upper amphibolite to granulite grade. Posttectonic granitoids of the Cullen Batholith intruded the Pine Creek Orogen between 1.84 and 1.80 Ga and produced thermal metamorphic aureoles in country rocks that overprinted regional metamorphic mineral assemblages. Rift-related felsic volcanic rocks were extruded unconformably over deformed sequences of the Pine Creek Orogen at approximately 1.83 Ga. These volcanic rocks are overlain by a thick succession of mainly fluviatile sandstone of the Katherine River Group, McArthur Basin (McKay and Miezitis, 2001; McCready et al., 2004; Sener, 2004; Lally and Bajwah, 2006; Cawood and Korsch, 2008; Pirajno and Bagas, 2008; Rajesh, 2008).

The Pine Creek Orogen is one of the world's premier uranium mineralized belts. It contains major unconformity-related uranium deposits such as Ranger (c. 184,000 t U_3O_8 at 0.17 to 0.34% U_3O_8), Jabiluka (163,000 t U_3O_8 at 0.53% U_3O_8) and Nabarlek (c. 11,000 t U_3O_8 at 1.95% U_3O_8) that occur in three key areas: the Alligator Rivers, South Alligator Valley, and Rum Jungle uranium fields. Uranium was first discovered in 1949 when a local prospector recognized torbernite in outcrops near the township of Batchelor and within what is now known as the Rum Jungle uranium field. This find lead to the discovery of the Whites uranium deposit, and triggered systematic search for uranium in the Pine Creek Orogen that was initially led by the

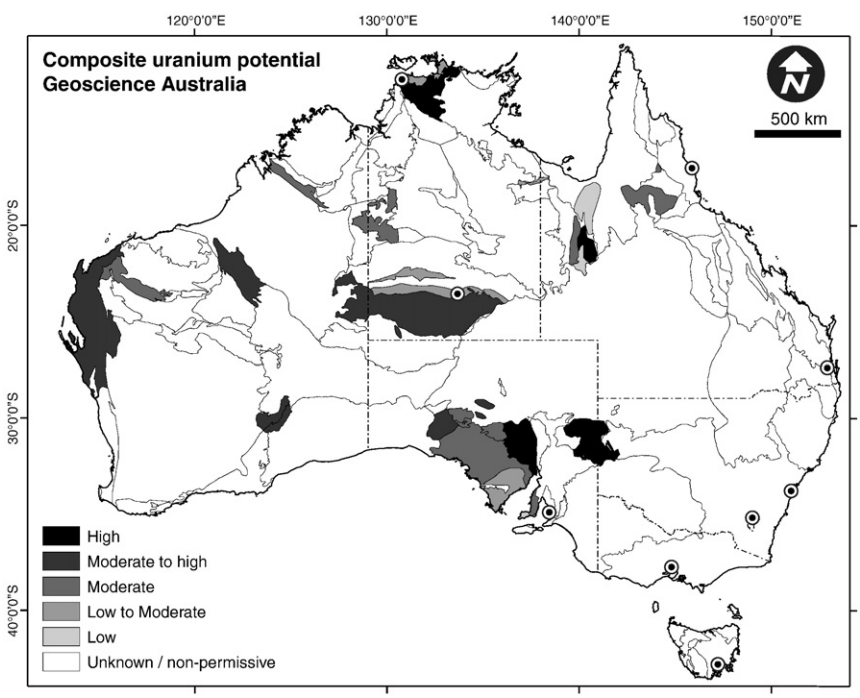

Fig. 10. Composite uranium potential map of the Australian continent modified after Geoscience Australia (www.australianminesatlas.gov.au/?site=atlas; last accessed on 12 June 2010). It is important to note that (1) this map illustrates the potential for unconformity-related, sandstone and breccia complex uranium deposits only, and (2) the highest level of potential for any of the three deposit types is shown for those areas where the potential for more than one of the three uranium deposit types overlap (Subash Jaireth, written communication, 2010). This map provides the only uranium prospectivity information (copyright by the Commenwealth of Australia, 2008) at the broad-regional to continent scale that is currently available in the public domain.

Australian Bureau of Mineral Resources. In 1953 the Bureau of Mineral Resources located Coronation Hill in the South Alligator Valley uranium field, whilst exploration by private sector companies resulted in the 1972 to 1973 discoveries of Ranger, Koongarra, Nabarlek and Jabiluka in the Alligator Rivers uranium field (McKay and Miezitis, 2001; Lally and Bajwah, 2006).

The Pine Creek Region contains several uranium fields with significant unconformity-related uranium deposits, most of which are located in the well-endowed Alligator Rivers uranium field (Jaireth and Huston, 2010). Given the many decades of uranium exploration in this region and related research, the key uranium mineralizing processes are well understood and prospective settings and rock types (e.g., Lower Cahill Formation, Whites Formation) well known (McKay and Miezitis, 2001; Lally and Bajwah, 2006; Rajesh, 2008; Skirrow et al., 2009a). The Pine Creek Region combines all ingredients required to form unconformity-related uranium deposits: (1) Unconformities that separate reduced basement rocks from overlying oxidized intracratonic basin sequences; (2) aquifers and permeable structures that permit fluid migration; (3) regional compression (i.e., basin inversion, active thrusting, and driving force for fluid migration) prior to and during uranium mineralization; and (4) mixing of oxidized basinal brines with reduced fluids or sites where oxidized basinal brines could interact with reduced strata (e.g., graphite-bearing schist). Hence, probability values of 1.0 were assigned to all critical mineralization processes (i.e., $P_{Mineralization}$ of 1.0). Given the high probability of occurrence of additional, potentially high-grade unconformity-related uranium deposits, the Pine Creek Region also scored a very high quality ranking of 10.0 (Fig. 5e, Table 3e). However, due to the relative maturity of this region, the best chance for discovery of new unconformity-related uranium deposits possibly exists where prospective rocks are under thin cover.

At the time of the manual uranium prospectivity analysis, the Pine Creek Region was extremely heavily tenemented and only small parcels of ground were available that are prospective for unconformity-related uranium deposits. Most of these parcels appeared to be vacant because of their locations next to nature reserves, national parks and water reservoirs or in areas with large numbers of underlying landholders.

3.3.2. King Leopold Region (Western Australia)

The King Leopold Region (Fig. 4b) covers an area of 12,000 km^2. It largely coincides with the King Leopold Orogen, a NW–SE-striking Paleoproterozoic mountain belt consisting of metasedimentary and igneous rocks of the Hooper Complex and deformed margins of the Speewah Basin and overlying Kimberley Basin. The Hooper Complex includes metamorphosed turbiditic sandstone, siltstone, mudstone, and felsic volcanic rocks of the Marboo Formation (c. 1.87 to 1.86 Ga) and metasedimentary rocks, anatectic gneiss and migmatite of the Mount Joseph Migmatite. It also includes dacitic to rhyolitic ignimbrites, minor lava flows, lapilli tuff, and volcanogenic sedimentary rocks of the Whitewater Volcanics (c. 1.85 Ga) that unconformably overlie the Marboo Formation, cogenetic high-level porphyries, granitoids and gabbro of the syntectonic Paperbark Supersuite (c. 1.87 to 1.85 Ga), and layered mafic sills of the Ruins Dolerite that cut the Marboo Formation (Hassan, 2004). The Hooper Complex is unconformably overlain by Paleoproterozoic sedimentary and volcanic rocks of the Speewah Group and unconformably overlying Kimberley Group. Both groups postdate the 1.87 to 1.85 Ga Hooper Orogeny (D1: layer-parallel foliation and greenschist facies metamorphism; D2: upright open to tight folding and greenschist to granulite facies metamorphism). The Speewah Group (i.e., O'Donnell Formation, Tunganary Formation, Valentine Siltstone (dated at c. 1.83 Ga), Lansdowne Arkose, Luman Siltstone, and Bedford Sandstone) was deposited during a transgressive–regressive cycle with basal fluviatile sandstone passing into or alternating with shallow-marine silt- and mudstone that, in turn, is overlain by another sequence of fluviatile sandstone. The Kimberley Group (King Leopold Sandstone, Carson Volcanics, Warton Sandstone, Elgee Siltstone, Pentecost Sandstone, Yampi Formation) is interpreted to have been deposited within a broad, semi-enclosed, shallow-marine basin with fluvial channels, tidal flats and shallow lagoons. Given the different sedimentary facies and inferred depositional environment, the Speewah and Kimberley groups are considered to have been deposited in separate basins. At approximately 1.79 Ga, the Speewah and Kimberley groups were intruded by massive dolerite sills and granophyres of the Hart Dolerite (Hassan, 2004).

There are no known unconformity-related uranium deposits in the King Leopold Region. However, uranium exploration in the Kimberley and Speewah basins between 1968 and 1987 (McKay and Miezitis, 2001; Whinnen Resources Limited, 2007) located several accumulations of secondary uranium minerals (e.g., Juno and Jupiter) at the base of the O'Donnell Formation (Speewah Group), directly above the unconformity that separates the Speewah Group from the underlying igneous and metamorphic rocks of the Hooper Complex. These secondary uranium minerals, which occur as impregnations in the rock matrix and on joint and fracture surfaces, have been interpreted by explorers as potential vectors to primary uranium mineralization in the basement (e.g., Whinnen Resources Limited, 2007). Rock chip sampling by U3O8 Limited (2010) at and near the unconformity between the O'Donnell Formation (Speewah Group) and Whitewater Volcanics (Lamboo Complex) in the neighboring, geologically similar Halls Creek Region (Hassan, 2000) returned anomalous uranium values of up to 2.06% U_3O_8. These results further corroborate the uranium potential of the unconformity at the base of the Speewah Group, both in the Halls Creek and King Leopold regions.

The King Leopold Region comprises a number of ingredients required to form unconformity-related uranium deposits (Table 3f): (1) Uranium-enriched Proterozoic basement rocks (Schofield, 2009a,b,c,d); (2) a significant Proterozoic unconformity that separates igneous and metamorphic basement rocks from overlying sedimentary sequences; and (3) evidence for uranium enrichment of sedimentary rocks immediately above this unconformity. However, little information is available with respect to the make-up of the Speewah Basin, availability of fluids to transport uranium, and redox gradients in the basin or basement. Given this uncertainty, the ranking of the King Leopold Region ($P_{Mineralization} = 0.75$) is significantly lower than that of the Pine Creek Region ($P_{Mineralization} = 1.00$) (Fig. 5e), although the quality ranking of the King Leopold Region (i.e., 7.50) is comparatively high given the potential for discovery of unconformity-related uranium deposits.

At the time of the manual uranium prospectivity analysis, the King Leopold Region was heavily tenemented. However, substantial parcels of ground were available along the prospective unconformity that separates the Speewah Group from the underlying Hooper Complex.

4. Discussion

4.1. New uranium deposit classification scheme

The new uranium deposit classification scheme introduced here is structured according to the widely accepted petroleum (Magoon and Dow, 1994) and mineral (Woodall, 1983; Wyborn et al., 1994; Knox-Robinson and Wyborn, 1997; Lord et al., 2001; Kreuzer et al., 2008) systems approaches. In this newly proposed scheme, the 14 principal uranium deposit types recognized by the International Atomic Energy Agency (2000) are grouped based on similarity of genetic processes, environments of ore formation and mappable ingredients (also known as exploration criteria). As such, this scheme is not a purely scientific classification scheme such as the recent novel proposals by Cuney (2009: deposit types grouped with respect to the main

fractionation processes along the geological cycle) and Skirrow et al. (2009a: deposit types grouped according to fluid compositions). Rather, it is a practical scheme that serves the purpose of exploration targeting on the broad-regional to continent scale. The new uranium systems models are simplified, flexible, and have internally consistent structures that not only emphasize depositional but also source and transport criteria, which are key parameters for area selection at the regional to continent scale (McCuaig et al., 2010). As such, they satisfy a fundamental principle of conceptual targeting: mineral deposits are part of much more extensive systems of energy and mass flux, and hence targeting must be carried out at global through to regional scales (Hronsky, 2004; Hronsky and Groves, 2008).

4.2. GIS-assisted manual versus GIS-driven automated prospectivity analysis

Manual approaches to mineral prospectivity analysis are seldom published (one of the rare examples is Penney et al., 2004) even though this type of prospectivity analysis is widely practiced in the minerals industry (Porwal and Kreuzer, 2010). Automated GIS-driven approaches, on the other hand, have been widely published, and over the past decade have gained broader acceptance and yielded successful results at a variety of scales (e.g., Bonham-Carter, 1994; Knox-Robinson, 2000; Harris et al., 2001; Bougrain et al., 2003; Brown et al., 2003; Porwal et al., 2003, 2006; Billa et al., 2004; Carranza, 2004; Nykänen and Ojala, 2007; Feltrin, 2008; Nykänen et al., 2008; Partington, 2008). Given the growing success, expanding capabilities and relative objectivity of automated prospectivity analysis, a common response may be why bother doing manual analyses?

The answer to this question lies in the current limitations of sophisticated computer-based mineral potential mapping techniques, which: (1) require input data that are unbiased, in a consistent format and preferably at similar scales; (2) cannot integrate cognitive concepts and literature information that are not in a spatial format; (3) cannot readily account for the timing of geological events and processes unless data have been processed appropriately; and (4) cannot readily deal with areas where the targeted geology is under cover unless geophysical interpretations are available.

Given that the human mind is capable of lateral thinking (De Bono, 1970) it is able to discern data errors much more efficiently than a computer. Hence, there is currently no substitute for the manual approach in situations where prospectivity analysis is carried out over areas where the target geology is poorly exposed or under cover, or where relevant datasets are not available, spatial information is limited, or input data are inconsistent or contain errors (Porwal and Kreuzer, 2010). However, the human brain cannot handle complex situations without simplifying them (e.g., Simon, 1983). This process can lead to heuristics and may introduce significant bias and errors of judgment (e.g., Tversky and Kahneman, 1974; Kahneman, 2003; Bond et al., 2007).

In our opinion, the best possible approach to a complex, continent-wide prospectivity analysis is to harness the strengths of both manual and automated approaches (Fig. 9). These approaches are complementary in that they essentially address each other's limitations, a thesis that is further investigated and discussed in a companion paper that will be submitted in early 2011. However, it is important that the manual analysis be undertaken first as to avoid anchoring to the automated analysis.

4.3. Scope of the manual uranium prospectivity analysis

There is little information in the public domain about the uranium potential of Australia at the broad-regional to continent scale, and it does not discriminate between the various types of uranium deposits (Fig. 10). As such, this study delivers a fresh look at the uranium prospectivity of the Australian continent because it considers all uranium deposit types known in Australia and covers geological regions that have never been publicly assessed for their uranium potential.

The approach presented in this paper provides a framework for GIS-assisted assessment of mineral potential. As such, this methodology is directly relevant to area selection (or exploration targeting) in which geological concepts are applied to commonly pre-existing datasets in order to make a subjective spatial prediction of mineral deposit occurrence (Hronsky, 2004; Hronsky and Groves, 2008). According to Penney et al. (2004), exploration decision-making (such as area selection) has for decades been an area of great subjectivity that traditionally relied on personal experience and intuition. Penney et al. (2004) also noted that no widely accepted methodologies have been developed to assist exploration decision-making.

Consciously or subconsciously, many exploration geoscientists follow steps or methods in the application of the targeting process that are similar to those presented in this paper (cf. McCuaig et al., 2007). However, few approaches have been formalized or published, a notable exception being a global-scale exploration risk analysis technique to determine the best mineral belts for zinc exploration by Penney et al. (2004) and a recent assessment of the hydrothermal nickel potential of Tasmania by González-Álvarez et al. (2010). Hence, one aim in our approach to manual prospectivity analysis was developing a semi-quantitative, probabilistic matrix-based structure that is amenable to exploration targeting at various scales (cf. McCuaig et al., 2010), can handle situations where information is missing and facilitates easy modification and updating, whilst also promoting consistency, reproducibility and transparency.

5. Conclusions

The following conclusions can be drawn from the GIS-assisted manual uranium prospectivity analysis described in this paper:

1. This study delivers a fresh look at the uranium prospectivity of the Australian continent because it considers all uranium deposit types known in Australia and covers geological regions that have never been publicly assessed for their uranium potential.
2. The newly proposed uranium systems models (i.e., surficial, sedimentary, igneous-related, metamorphic/metasomatic, unconformity-related, and vein-related) provide a pragmatic framework for prospectivity analysis at the broad-regional to continent scale based on the mineral systems approach.
3. The approach taken in this study, namely to link the mineral systems concept to a semi-quantitative, probabilistic and flexible matrix, facilitates easy modification and updating of technical assessments, whilst also promoting transparency, objectivity and reproducibility.
4. Maps based on the numerical results of the technical, quality and opportunity ranking schemes developed and applied in this study highlight the geological regions with the highest probability of occurrence of a particular uranium deposit type, greatest potential for occurrence of high-quality uranium deposits, and greatest opportunity of available, prospective ground. As such, the various ranking schemes help to inform area selection decisions and detailed follow-up studies, and focus time and resources.
5. The geological regions with the highest quality ranking are the Ashburton, Broken Hill, Litchfield, McArthur, Money Shoal, Murphy, Paterson, Pine Creek and Northeast Tasmania regions (quality ranking of 10.0), the Gawler and Polda regions (quality ranking of 9.0), and the Amadeus, Georgetown, Stuart, Tanami regions (quality ranking of 8.1). In our opinion and according to the data assessed in this study, the above regions have the greatest potential for discovery of potentially recoverable uranium resources. Most of these regions contain known unconformity-related or sandstone-hosted uranium deposits, although some of them are pure conceptual plays and have received relatively little attention in terms of uranium exploration.

Acknowledgements

The authors acknowledge project funding by Regalpoint Resources Ltd and thank the directors for permission to publish aspects of a uranium prospectivity study undertaken on behalf of the company. Intierra Resource Intelligence is thanked for access to their Minmet Global database. The manuscript greatly benefited from thorough reviews by David Groves and an anonymous referee, and skilled editorial handling by Frank Bierlein.

References

Abeysinghe, P.B., 2003. Mineral occurrences and exploration activities in the Arunta–Musgrave area. Geological Survey of Western Australia Record 2002/9 33 pp.
Ahmad, R., Wilson, C.J.L., 1981. Uranium and boron distributions related to metamorphic microstructure — evidence for metamorphic fluid activity. Contributions to Mineralogy and Petrology 76, 24–32.
Allard, B., Arsenie, I., Hakansson, K., Karlsson, S., Ahlberg, A.C., Lundgren, T., Collin, M., Rasmuson, A., Strandell, E., 1991. Effects of weathering on metal releases from an engineered deposit for alum shale leaching residues. Water, Air and Soil Pollution 57–58, 431–440.
Alley, N.F., 1998. Cainozoic stratigraphy, palaeoenvironments and geological evolution of the Lake Eyre Basin. Palaeogeography, Palaeoclimatology, Palaeoecology 144, 239–263.
Altschuler, Z.S., Clarke, R.S., Young, E.J., 1958. Geochemistry of uranium in apatite and phosphorite. Geological Survey Professional Paper 314-D, 45–90.
Anand, R.R., Paine, M., 2002. Regolith geology of the Yilgarn Craton, Western Australia: implications for exploration. Australian Journal of Earth Sciences 49, 3–162.
Ashley, P.M., 1984. Sodic granitoids and felsic gneisses associated with uranium–thorium mineralisation, Crockers Well, South Australia. Mineralium Deposita 19, 7–18.
Bain, J.H.C., Draper, J.J., 1997. North Queensland Geology. Australian Geological Survey Organisation Bulletin 240 600 pp.
Basson, I.J., Greenway, G., 2004. The Rössing uranium deposit: a product of late-kinematic localization of uraniferous granites in the central zone of the Damara Orogen, Namibia. Journal of African Earth Sciences 38, 413–435.
Berning, J., Cooke, R., Hiemstra, S.A., Hoffman, U., 1976. The Roessing uranium deposit, South West Africa. Economic Geology 71, 351–368.
Billa, M., Cassard, D., Lips, A.L.W., Bouchot, V., Tourlière, B., Stein, G., Guillou-Frottier, G., 2004. Predicting gold-rich epithermal and porphyry systems in the central Andes with a continental-scale metallogenic GIS. Ore Geology Reviews 25, 39–67.
Bond, C.E., Gibbs, A.D., Shipton, Z.K., Jones, S., 2007. What do you think this is? "Conceptual uncertainty" in geosciences interpretation. GSA Today 17, 4–10.
Bonham-Carter, G.F., 1994. Geographic Information Systems for Geoscientists: Modelling with GIS. Pergamon Press, Oxford. 398 pp.
Bougrain, L., Gonzalez, M., Bouchot, V., Cassard, D., Lips, A.L.W., Alexandre, F., Stein, G., 2003. Knowledge recovery for continental-scale mineral exploration by neural networks. Natural Resources Research 12, 173–181.
Bowie, S., 1979. The mode of occurrence and distribution of uranium deposits. Philosophical Transactions of the Royal Society of London, Series A: Mathematical and Physical Sciences 291, 289–300.
Brown, W., Groves, D.I., Gedeon, T., 2003. Use of fuzzy membership input layers to combine subjective geological knowledge and empirical data in a neural network method for mineral-potential mapping. Natural Resources Research 12, 183–200.
Brugger, J., Long, N., McPhail, D.C., Plimer, I., 2005. An active magmatic hydrothermal system; the Paralana hot springs, northern Flinders Ranges, South Australia. Chemical Geology 222, 35–64.
Buntebarth, G., 1976. Distribution of uranium in intrusive bodies due to combined migration and diffusion. Earth and Planetary of Science Letters 32, 84–90.
Butt, C.R.M., Gray, D.J., 2007. Palaeochannel uranium in southern Western Australia: déjà vu all over again. In: Bierlein, F.P., Knox-Robinson, C.M. (Eds.), Proceedings of Geoconferences (WA) Inc Kalgoorlie '07 Conference, 25–27 September 2007. Kalgoorlie, Western Australia, pp. 115–117.
Butt, C.R.M., Mann, A.W., Horwitz, R.C., 1984. Regional setting, distribution and genesis of surficial uranium deposits in calcretes and associated sediments in Australia. Surficial Uranium Deposits. International Atomic Energy Agency, Vienna, IAEA-TECDOC-322, pp. 121–128.
Cameron, E., 1990. Yeelirrie uranium deposit. In: Hughes, F.E. (Ed.), Geology of the Mineral Deposits of Australia and Papua New Guinea. Monograph, 14. Australasian Institute of Mining and Metallurgy, Melbourne, pp. 1625–1629.
Cameron, E., Mazzucchelli, R.H., Robbins, T.W., 1980. Yeelirrie calcrete uranium deposit, Murchison region, WA. Journal of Geochemical Exploration 12, 350–353.
Carranza, E.J.M., 2004. Weights of evidence modeling of mineral potential: a case study using small number of prospects, Abra, Philippines. Natural Resources Research 13, 173–187.
Cartwright, I., 1994. The two-dimensional pattern of metamorphic fluid flow at Mary Kathleen, Australia: fluid focusing, transverse dispersion, and implications for modeling fluid flow. Journal of the Mineralogical Society of America 79, 526–535.
Cassidy, K.F., Champion, D.C., Krapez, B., Barley, M.E., Brown, S.J.A., Blewett, R.S., Groenewald, P.B., Tyler, I.M., 2006. A revised geological framework for the Yilgarn Craton, Western Australia. Geological Survey of Western Australia, Record 2006/08, 8 p.
Cawood, P.A., Korsch, R.J., 2008. Assembling Australia: Proterozoic building of a continent. Precambrian Research 166, 1–38.
Chabiron, A., Cuney, M., Poty, B., 2003. Possible uranium sources for the largest uranium district associated with volcanism: the Streltsovska caldera (Transbaikalia, Russia). Mineralium Deposita 38, 127–140.
Cotton, T.B., Scardigno, M.F., Hibburt, J.E. (Eds.), 2006. The Petroleum Geology of South Australia, Volume 2: Eromanga Basin. Second Edition, South Australia Department of Primary Industries and Resources, Petroleum Geology of South Australia Series. [http://www.pir.sa.gov.au/petroleum/access_to_data/petroleum_publications/petroleum_geology_of_south_australia/vol_2_-_eromaga_basin_2nd_edition; last accessed: 30 April 2010].
Coward, M.P., Spencer, R.M., Spencer, C.E., 1995. Development of the Witwatersrand Basin. Geological Society of South Africa Special Publication 95, 243–269.
Cuney, M., 2009. The extreme diversity of uranium deposits. Mineralium Deposita 44, 3–9.
Dahlkamp, F.J., 1978. Classification of uranium deposits. Mineralium Deposita 13, 83–104.
Dahlkamp, F.J., 1993. Uranium Ore Deposits. Springer, Berlin. 460 pp.
De Bono, E., 1970. Lateral Thinking: Creativity Step by Step. Harper and Row, New York. 304 pp.
de Broekert, P., Sandiford, M., 2005. Buried inset-valleys in the eastern Yilgarn Craton, Western Australia. Journal of Geology 113, 471–493.
Desert Energy Limited, 2008. Uranium mineralization discovered at Old Station West. Announcement to the Australian Securities Exchange, 28 November 2008, 9 p. [www.asx.com.au/asxpdf/20081128/pdf/31dx6k42101sc7.pdf; last accessed: 02 May 2010].
Douglas, G., Butt, C.R.M., Gray, D.J., 2003. Mulga rock uranium and multi-element deposits, Officer Basin, WA. In: Butt, C.R.M., Robertson, I.D.M., Scott, K.M., Cornelius, M. (Eds.), Regolith Expression of Australian Ore Systems: a Compilation of Case Histories with Conceptual Dispersion, Process and Exploration Models. Cooperative Research Centre for Landscape Environments and Mineral Exploration, Perth, pp. 415–418. [crcleme.org.au/RegExpOre/MulgaRock.pdf; last accessed: 20 March 2009].
The geology of South Australia, volume 2: the Phanerozoic. In: Drexel, J.F., Preiss, W.V. (Eds.), South Australia Geological Survey Bulletin, 54. 347 pp.
Duncan, R.Y., Wilde, A.R., Maas, R., Bassano, K., 2006. Geochronological constraints on tourmaline formation in the western fold belt of Mount Isa, Australia: evidence for large-scale metamorphism at 1.57 Ga? Precambrian Research 146, 120–137.
England, G.L., Rasmussen, B., Krapez, B., Groves, D.I., 2002. Palaeoenvironmental significance of rounded pyrite in siliciclastic sequences of the Late Archean Witwatersrand Basin: oxygen-deficient atmosphere or hydrothermal alteration? Sedimentology 49, 1133–1156.
Feltrin, L., 2008. Predictive modelling of prospectivity for Pb–Zn deposits in the Lawn Hill Region, Queensland, Australia. Ore Geology Reviews 34, 399–427.
Finch, W.I., 1992. Descriptive model of solution-collapse breccia pipe uranium deposits (Model 32e). In: Bliss, J.D. (Ed.), Developments in Mineral Deposit Modeling. U.S. Geological Survey Bulletin 2004, pp. 33–35.
Finch, W.I., 1996. Uranium provinces of North America — their definition, distribution, and models. U.S. Geological Survey Bulletin 2141 18 pp.
Finch, W.I., Davis, J.F., 1985. Geological environments of sandstone-type uranium deposits. International Atomic Energy Agency, Vienna, IAEA-TECDOC-328. 408 pp.
Frimmel, H.E., 2005. Archean atmospheric evolution: evidence from the Witwatersrand gold fields, South Africa. Earth Science Reviews 70, 1–46.
Fulwood, K.E., Barwick, R.E., 1990. Mulga rock uranium deposits, Officer Basin. In: Hughes, F.E. (Ed.), Geology of the Mineral Deposits of Australia and Papua New Guinea: Monograph, 14. Australasian Institute of Mining and Metallurgy, Melbourne, pp. 1621–1623.
Georgakopoulos, A., 2001. Trace elements in the Lava xylite / lignite deposit, Servia Basin, Northern Greece. Energy Sources 23, 143–156.
Goad, R.E., Mumin, J.A., Duke, N.A., Neale, K.L., Mulligan, D.L., Camier, W.J., 2001. The NICO and Sue-Dianne Proterozoic, iron oxide-hosted, polymetallic deposits, Northwest Territories: application of the Olympic Dam model in exploration. Exploration Mining Geology 9, 123–140.
González-Álvarez, I., Porwal, A.K., Beresford, S.W., McCuaig, T.C., Maier, W.D., 2010. Hydrothermal Ni prospectivity analysis of Tasmania, Australia. Ore Geology Reviews 38, 168–183.
Gow, P.A., Wall, V.J., Oliver, N.H.S., Valenta, R.K., 1994. Proterozoic iron oxide (Cu–U–Au–REE) deposits: further evidence of hydrothermal origins. Geology 22, 633–636.
Gregory, M.J., Wilde, A.R., Jones, P.A., 2005. Uranium deposits of the Mount Isa region and their relationship to deformation, metamorphism, and copper deposition. Economic Geology 100, 537–546.
Harris, J.R., Wilkinson, L., Heather, K., Fumerton, S., Bernier, M.A., Ayer, J., Dahn, R., 2001. Application of GIS processing techniques for producing mineral prospectivity maps — a case study: mesothermal Au in the Swayze Greenstone Belt, Ontario, Canada. Natural Resources Research 10, 91–124.
Hartleb, J.W.O., 1988. The Langer Heinrich uranium deposit; Southwest Africa/Namibia. Ore Geology Review 3, 277–287.
Hassan, L.Y., 2000. Mineral occurrences and exploration potential of the East Kimberley. Geological Survey of Western Australia Report 74 83 pp.
Hassan, L.Y., 2004. Mineral occurrences and exploration potential of the West Kimberley. Geological Survey of Western Australia Report 88 88 pp.
Haynes, D.W., Cross, K.C., Bills, R.T., Reed, M.H., 1995. Olympic Dam ore genesis; a fluid-mixing model. Economic Geology 90, 281–307.
Heier, K.S., 1979. The movement of uranium during higher grade metamorphic processes. Philosophic Transaction of the Royal Society of London 291, 413–421.
Hein, K.A.A., 2002. Geology of the Ranger uranium mine, Northern Territory, Australia: structural constraints on the timing of uranium emplacement. Ore Geology Reviews 20, 83–108.

Heinson, G.S., Direen, N.G., Gill, R.M., 2006. Magnetotelluric evidence for a deep-crustal mineralizing system beneath the Olympic Dam iron oxide copper–gold deposit, southern Australia. Geology 34, 573–576.
Hitzman, M.W., 2000. Iron oxide–Cu–Au deposits: what, where, when, and why. In: Porter, T.M. (Ed.), Hydrothermal Iron Oxide–Copper–Gold and Related Deposits: a Global Perspective. Australian Mineral Foundation, Adelaide, Australia, pp. 9–25.
Hitzman, M.W., Valenta, R.K., 2005. Uranium in iron oxide–copper–gold (IOGG) systems. Economic Geology 100, 1657–1661.
Hobday, D.K., Galloway, W.E., 1999. Groundwater processes and sedimentary uranium deposits. Hydrogeology 7, 127–138.
Hocking, R.M., Moors, H.T., van de Graaf, W.J.E., 1987. Geology of the Carnarvon Basin, Western Australia. Geological Survey of Western Australia Bulletin 133 289 pp.
Hofmann, B., Eikenberg, J., 1991. The Krunkelbach uranium deposit, Schwarzwald, Germany; correlation of radiometric ages (U–Pb, U–Xe–Kr, K–Ar, 230TH, 234U). Economic Geology 86, 1031–1049.
Hou, B., Fabris, A.J., Keeling, J.L., Fairclough, M.C., 2007a. Cainozoic palaeochannel-hosted uranium and current exploration methods, South Australia. MESA Journal 46, 34–39.
Hou, B., Zang, W., Fabris, A.J., Keeling, J.L., Stoian, L., Fairclough, M.C., 2007b. Palaeodrainage and Tertiary Coastal Barriers of South Australia. Digital Geological Map of South Australia, 1:2, 000, 000 Series, 1st Edition. CRC LEME and Geological Survey Branch, Primary Industries Resources South Australia. [crcleme.org.au/Pubs/ PubsOther/ palaeochannels_sa_map%20PIRSAJune07.pdf; last accessed: 10 May 2010].
Howard, P.F., Hough, M.J., 1979. On the geochemistry and origin of the D Tree, Wonarah, and Sherrin Creek phosphorite deposits of the Georgina Basin, northern Australia. Economic Geology 74, 260–284.
Hronsky, J.M.A., 2004. The science of exploration targeting. In: Muhling, J. (Ed.), University of Western Australia and Centre for Global Metallogeny Publication, 33, pp. 129–133.
Hronsky, J.M.A., Groves, D.I., 2008. Science of targeting: definition, strategies, targeting and performance measurement. Australian Journal of Earth Sciences 55, 3–12.
International Atomic Energy Agency, 2000. Methods of Exploitation of Different Types of Uranium Deposits. International Atomic Energy Agency, Vienna, IAEA-TECDOC-1174, 75 p.
Jackson, D.J., Andrew, R.L., 1990. Kintyre uranium deposit. In: Hughes, F.E. (Ed.), Geology of the Mineral Deposits of Australia and Papua New Guinea. Monograph, 14. Australasian Institute of Mining and Metallurgy, Melbourne, pp. 653–658.
Jaireth, S., Huston, D., 2010. Metal endowment of cratons, terranes and districts: insights from a quantitative analysis of regions with giant and super-giant deposits. Ore Geology Reviews 38, 288–303.
Jaireth, S., McKay, A., Lambert, I., 2008. Association of large sandstone uranium deposits with hydrocarbons. Geoscience Australia Ausgeo News 89 6 pp.
Jaireth, S., Clarke, J., Cross, A., 2010. Exploring for sandstone-hosted uranium deposits in paleovalleys and palaeochannels. Geoscience Australia Ausgeo News 97 5 pp.
Jefferson, C.W., Thomas, D.J., Gandhi, S.S., Ramaekers, P., Delaney, G., Brisbin, D., Cutts, C., Portella, P., Olson, R.A., 2007. Unconformity-associated uranium deposits of the Athabasca Basin, Saskatchewan and Alberta. In: Jefferson, C.W., Delaney, G. (Eds.), EXTECH IV: Geology and Uranium Exploration Technology of the Proterozoic Athabasca Basin, Saskatchewan and Alberta: Geological Survey of Canada Bulletin, 588, pp. 23–67.
Jones, R.M., Hillis, R.R., 2003. An integrated, quantitative approach to assessing fault-seal risk. AAPG Bulletin 87, 507–524.
Kahneman, D., 2003. A perspective on judgment and choice mapping bounded rationality. American Psychologist 58, 697–720.
Knox-Robinson, C.M., 2000. Vectorial fuzzy logic: a novel technique for enhanced mineral prospectivity mapping, with reference to the orogenic gold mineralisation potential of the Kalgoorlie terrane, Western Australia. Australian Journal of Earth Sciences 47, 929–941.
Knox-Robinson, C.M., Wyborn, L.A.I., 1997. Towards a holistic exploration strategy: using geographic information systems as tool to enhance exploration. Australian Journal of Earth Sciences 44, 453–463.
Kreuzer, O.P., Etheridge, M.A., Guj, P., McMahon, M.E., Holden, D.J., 2008. Linking mineral deposit models to quantitative risk analysis and decision-making in exploration. Economic Geology 103, 829–850.
Lally, J.H., Bajwah, Z.U., 2006. Uranium deposits of the Northern Territory. Northern Territory Geological Survey Report 20 87 pp.
Lambert, I., Jaireth, S., McKay, A., Miezitis, Y., 2005. Why Australia has so much uranium. Ausgeo News 80 4 pp.
Langford, F.F., 1974. A supergene origin for vein-type uranium ores in the light of the Western Australian calcrete–carnotite deposits. Economic Geology 69, 516–526.
Langwaldt, J., 2006. Microbial interaction with black shale ores — from natural to industrial bioleaching. Geological Survey of Finland [en.gtk.fi/export/sites/default/ Research/Sustainable_Use/Langwaldt240506.pdf; last accessed 25 April 2009].
Law, J., Phillips, G.N., 2006. Witwatersrand gold–pyrite–uraninite deposits do not support a reducing Archean atmosphere. In: Kesler, S.E., Ohmoto, H. (Eds.), Evolution of Early Earth's Atmosphere, Hydrosphere, and Biosphere — Constraints from Ore Deposits: Geological Society of America Memoir, 198, pp. 121–141.
Lewan, M.D., Buchardt, B., 1989. Irradiation of organic matter by uranium decay in the Alum Shale, Sweden. Geochimica et Cosmochimica Acta 53, 1307–1322.
Lord, D., Etheridge, M.A., Willson, M., Hall, G., Uttley, P.J., 2001. Measuring exploration success: an alternative to the discovery-cost-per-ounce method of quantifying exploration success. Society of Economic Geologists Newsletter 45, 1 and 10–16.
Ludwig, K.R., Wallace, A.R., Simmons, K.R., 1985. The Schwartzwalder uranium deposit; II. Age of uranium mineralization and lead isotope constraints on genesis. Economic Geology 80, 1858–1871.
Magoon, L.B., Dow, W.G., 1994. The petroleum system. In: Magoon, L.B., Dow, W.G. (Eds.), The Petroleum System: From Source to Trap: American Association of Petroleum Geologists Memoir, 60, pp. 3–24.
Mann, A.W., Deutscher, R.L., 1978. Genesis principles for the precipitation of carnotite in calcrete drainages in Western Australia. Economic Geology 73, 1724–1737.
Marshall, L.J., Oliver, N.H.S., Davidson, G.J., 2006. Carbon and oxygen isotope constraints on fluid sources and fluid–wallrock interaction in regional alteration and iron-oxide–copper–gold mineralisation, eastern Mt Isa Block, Australia. Mineralium Deposita 41, 429–452.
Mashkovtsev, G.A., Kislyakov, Y.M., Miguta, A.K., Modnikov, I.S., Shchetochkin, V.N., 1995. Uranium deposits: main types and concepts for detection. Changes and Events in Uranium Deposit Development, Exploration, Resources, Production and the World Supply-Demand Relationship. International Atomic Energy Agency and OECD Nuclear Energy Agency, Vienna, IAEA-TECDOC-961, pp. 297–306.
McCready, A.J., Stumpfl, E.F., Lally, J.H., Ahmad, M., Gee, R.D., 2004. Polymetallic mineralization at the Browns deposit, Rum Jungle mineral field, Northern Territory, Australia. Economic Geology 99, 257–277.
McCuaig, T.C., Kreuzer, O.P., Brown, W.M., 2007. Fooling ourselves — dealing with model uncertainty in a mineral systems approach to exploration. Mineral Exploration and Research: Digging Deeper: Proceedings of the 9th Biennial SGA Meeting, Dublin, pp. 1435–1438.
McCuaig, T.C., Beresford, S.W., Hronsky, J.M.A., 2010. Translating the mineral systems approach into an effective exploration targeting system. Ore Geology Reviews 38, 128–138.
McKay, A.D., Miezitis, Y., 2001. Australia's uranium resources, geology and development of deposits. Australian Geological Survey Organisation — Geoscience Australia Mineral Resource Report 1 184 pp.
McKay, A.D., Miezitis, Y., Jaireth, S., 2009. Australian Uranium Resources, May 2009 Edition, 1:10, 000, 000 Scale Map. Geoscience Australia [www.ga.gov.au/servlet/ BigObjFileManager?bigobjid=GA15495; last accessed: 15 May 2010].
McMillan, R.H., 1996. "Classical" U veins. Geological survey of Canada. British Columbia Energy and Minerals Division, Special Publication 93–96.
Mernagh, T.P., Wyborn, L.A.I., Jagodzinski, E.A., 1998. Unconformity-related U–Au–platinum-group-element deposits. Journal of Australian Geology and Geophysics 17, 197–205.
Min, M., Zheng, D., Shen, B., Wen, G., Wang, X., Gandhi, S.S., 1997. Genesis of the Sanbaqi deposit: a paleokarst-hosted uranium deposit in China. Mineralium Deposita 32, 505–519.
Myers, J.S., 1993. Precambrian history of the West Australian Craton and adjacent orogens. Annual Review of Earth and Planetary Sciences 21, 453–481.
O.E.C.D. Nuclear Energy Agency, International Atomic Energy Agency, 2005. Uranium 2005: Resourced, Production and Demand ("Red Book"). OECD Publications, Paris. 388 pp.
Nykänen, V., Ojala, V.J., 2007. Spatial analysis techniques as successful mineral-potential mapping tools for orogenic gold deposits in the northern Fennoscandian Shield, Finland. Natural Resources Research 16, 85–92.
Nykänen, V., Groves, D.I., Ojala, V.J., Eilu, P., Gardoll, S.J., 2008. Reconnaissance-scale conceptual fuzzy-logic prospectivity modelling for iron oxide copper–gold deposits in the northern Fennoscandian Shield, Finland. Australian Journal of Earth Sciences 55, 25–38.
Oliver, N.H.S., Pearson, P.J., Holcombe, R.J., Ord, A., 1999. Mary Kathleen metamorphic-hydrothermal uranium-rare earth element deposit: ore genesis and numerical model of coupled deformation and fluid flow. Australian Journal of Earth Sciences 46, 467–484.
Pana, D., Creaser, R.A., Muehlenbachs, K., Wheatley, K., 2007. Basement geology in the Alberta portion of the Athabasca Basin: context for the Maybelle River area. In: Jefferson, C.W., Delaney, G. (Eds.), EXTECH IV: Geology and Uranium Exploration Technology of the Proterozoic Athabasca Basin, Saskatchewan and Alberta: Geological Survey of Canada Bulletin, 588, pp. 135–153.
Parkin, L.W., Glasson, K.R., 1954. The geology of the Radium Hill mine. Economic Geology 49, 815–825.
Partington, G., 2008. Prospectivity analysis in action: the Auzex Resources Ltd (AZX) story as applied to granite related mineral systems in Eastern Australia and New Zealand. Australian Earth Sciences Convention, Perth, July 20 to July 24, p. 195.
Penney, S.R., Allen, R.M., Harrisson, S., Lees, T.C., Murphy, F.C., Norman, A.R., Roberts, P.A., 2004. A global-scale exploration risk analysis technique to determine the best mineral belts for exploration. Transactions of the Institute of Mining and Metallurgy, Section B: Applied Earth Science 113, 183–196.
Pirajno, F., Bagas, L., 2008. A review of Australia's Proterozoic mineral systems and genetic models. Precambrian Research 166, 54–80.
Porwal, A.K., Kreuzer, O.P., 2010. Introduction to the Special Issue: mineral prospectivity analysis and quantitative resource estimation. Ore Geology Reviews 38, 121–127.
Porwal, A.K., Carranza, E.J.M., Hale, M., 2003. Knowledge-driven and data-driven fuzzy models for predictive mineral potential mapping. Natural Resources Research 12, 1–25.
Porwal, A.K., Carranza, E.J.M., Hale, M., 2006. Bayesian network classifiers for mineral potential mapping. Computers and Geosciences 32, 1–16.
Psilovikos, A., Karistineos, N., 1986. A depositional sedimentary model for the Neogene uraniferous lignites of the Serres Graben, Greece. Palaeogeography, Palaeoclimatology, Palaeoecology 56, 1–16.
Rajesh, H.M., 2008. Mapping Proterozoic unconformity-related uranium deposits in the Rockhole area, Northern Territory, Australia using landsat ETM+. Ore Geology Reviews 33, 382–396.
Ruzicka, V., 1993. Vein uranium deposits. Ore Geology Reviews 8, 247–276.
Sanford, R., 1990. Hydrogeology of an ancient arid closed basin: implications for tabular sandstone-hosted uranium deposits. Geology 18, 1099–1102.

Schofield, A., 2009a. Uranium content of igneous rocks of australia 1:5, 000, 000 maps: explanatory notes and discussion. Geoscience Australia Record 2009/17, 20 p.
Schofield, A., 2009b. Uranium content of igneous rocks of Australia: map 1: igneous rock type: surface geology, 1:500, 000 scale. Geoscience Australia [www.ga.gov.au/servlet/BigObjFileManager?bigobjid=GA14269; last accessed: 15 May 2010].
Schofield, A., 2009c. Uranium content of igneous rocks of Australia: map 2: average uranium abundance: surface geology, 1:500, 000 scale. Geoscience Australia [www.ga.gov.au/servlet/BigObjFileManager?bigobjid=GA14270; last accessed: 15 May 2010].
Schofield, A., 2009d. Uranium content of igneous rocks of Australia: map 3: average abundance: solid geology, 1:500, 000 scale. Geoscience Australia [www.ga.gov.au/servlet/BigObjFileManager?bigobjid=GA14271; last accessed: 15 May 2010].
Seat, Z., Beresford, S.W., Grguric, B.A., Waugh, R.S., Hronsky, J.M.A., Gee, M.A.M., Groves, D.I., Mathison, C.I., 2007. Architecture and emplacement of the Nebo-Babel gabbronorite-hosted magmatic Ni–Cu–PGE sulphide deposit, West Musgrave, Western Australia. Mineralium Deposita 42, 551–581.
Sener, A.K., 2004. Characteristics, distribution and timing of gold mineralisation in the Pine Creek Orogen, Northern Territory, Australia. Unpublished PhD thesis, Centre for Global Metallogeny, The University of Western Australia, 243 p.
Simon, H.A., 1983. Search and reasoning in problem solving. Artificial Intelligence 21, 7–29.
Skirrow, R.G., 2009. New views of Australia's uranium mineral systems. Ausgeo News 95 4 pp.
Skirrow, R.G., Walshe, J.L., 2002. Reduced and oxidized Au–Cu–Bi iron oxide deposits of the Tennant Creek Inlier; Australia: an integrated geologic and chemical model. Economic Geology 97, 1167–1202.
Skirrow, R.G., Jaireth, S., Huston, D.L., Bastrakov, E.N., Schofield, A., van der Wielen, S.E., Barnicoat, A.C., 2009a. Uranium mineral systems: processes, exploration criteria and a new deposit framework. Geoscience Australia Record 2009/20 49 pp.
Skirrow, R.G., Bastrakov, E.N., Britt, A.F., Cross, A., Hill, S.M., Hore, S.B., Jaireth, S., Le Gleuher, M., Schofield, A., van der Wielen, S.E., 2009b. Uranium ore-forming systems of the Lake Frome region, South Australia: regional spatial controls and exploration criteria. Geoscience Australia Record 2009/40 151 pp.
Solomon, M., Groves, D.I., 2000. The geology and origin of Australia's mineral deposits (reprinted with additional material): Centre for Ore Deposits Research, University of Tasmania, and Centre for Global Metallogeny, University of Western Australia Publication 32, 1002 p.
Spirakis, C., 1996. The roles of organic matter in the formation of uranium deposits in sedimentary rocks. Ore Geology Reviews 11, 53–69.
Thomas, D., Zaluski, G., Brisbin, D., Drever, G., 2006. Uranium deposit models, with an emphasis on sedimentary-associated types. Presentation by Cameco Corporation at the Centre for Exploration Targeting, University of Western Australia, Perth, Australia, 29 November 2006.
Toro Energy Limited, 2008. Napperby uranium project, Australian Uranium Conference Fremantle — July 2008. Announcement to the Australian Securities Exchange, 23 July 2008, 21 p. [www.asx.com.au/asxpdf/20080723/pdf/31b9gp33k94b2c.pdf; last accessed: 15 May 2010].
Tversky, A., Kahneman, D., 1974. Availability: a heuristic for judging frequency and probability. Cognitive Psychology 5, 207–232.
U3O8 Limited, 2010. Quarterly report for the three month period ending 31 March 2010. Announcement to the Australian Securities Exchange, 22 April 2010, 16 p [www.asx.com.au/asxpdf/20100422/pdf/31px9gtx1t89sq.pdf; last accessed: 02 May 2010].
Uranium Equities Limited, 2008. Agreement reached with Cameco Australia Pty Ltd to farm into the Lake Blanche project. Announcement to the Australian Securities Exchange, 27 November 2008, 2 p [www.asx.com.au/asxpdf/20081127/pdf/31dw1022rsv04v.pdf; last accessed: 01 May 2010].
Van Gosen, B.S., Wenrich, K.J., 1989. Ground magnetometer surveys over known and suspected breccia pipes on the Coconino Plateau, northwestern Arizona. U.S. Geological Survey Bulletin 1683-C 31 pp.
Vennemann, T.W., Kesler, S.E., O'Neil, J.R., 1992. Stable isotope compositions of quartz pebbles and their fluid inclusions as tracers of sediment provenance: implications for gold- and uranium-bearing quartz pebble conglomerates. Geology 20, 837–840.
Vigar, A., Jones, D.G., 2005. Technical report on the mining leases covering the Ben Lomond uranium–molybdenum deposit, Queensland, Australia. Technical Report to Maple Minerals Corporation, 42 p [www.megauranium.com/UserFiles/File/Ben Lomond 43-101.pdf; last accessed: 20 March 2009].
Wall, V.J., 2006. Unconformity-related uranium systems — up, down, sideways. In: Australia's Uranium 2006: World Leadership in Exploration, Resources, Mining, Processing and Regulation, 10 to 11 July 2006, Adelaide, South Australia. Presentations and Abstract Volume [CD-ROM], Australasian Institute of Mining and Metallurgy, Carlton, Victoria.
Wallace, A.R., Karlson, R.C., 1985. The Schwartzwalder uranium deposit; I. Geology and structural controls on mineralization. Economic Geology 80, 1842–1857.
Wallace, A.R., Whelan, J.F., 1986. The Schwartzwalder uranium deposit; III. Alteration, vein mineralization, light stable isotopes, and genesis of the deposit. Economic Geology 81, 872–888.
Watson, P., 1998. A process for estimating geological risk of petroleum prospects. Journal of the Australian Petroleum Production and Exploration Association 38, 577–583.
Wenrich, K.J., 1985. Mineralization of breccia pipes in northern Arizona. Economic Geology 80, 1722–1735.
Wenrich, K.J., 1986. Geochemical exploration for mineralized breccia pipes in northern Arizona, U.S.A. Applied Geochemistry 1, 469–485.
Wenrich, K.J., Van Gosen, B.S., Finch, W.I., 2004. Solution-collapse breccias pipe U deposits (Model 32e). In: du Bray, E.A. (Ed.), Preliminary Compilation of Descriptive Geoenvironmental Mineral Deposit Models: U.S. Geological Survey Open-File Book, 95-831, pp. 244–251.
Whinnen Resources Limited, 2007. Prospectus. Australian Securities and Investments Commission Document Number 023066391, Lodgment Date: 14 March 2007, 91 p [www.whinnenresources.com.au/upload/pages/ipo-prospectus/whinnen-prospectus.pdf; last accessed: 02 May 2010].
Wilde, A., Wall, V.J., 1987. Geology of the Nabarlek uranium deposit, Northern Territory, Australia. Economic Geology 82, 1152–1168.
Williams, P.J., Pollard, P.J., 2003. Australian Proterozoic iron oxide–Cu–Au deposits: an overview with new metallogenic and exploration data from the Cloncurry district, northwest Queensland. Exploration and Mining Geology 10, 191–213.
Williams, P.J., Barton, M.D., Johnson, D.A., Fontbote, L., De Haller, A., Mark, G., Oliver, N.H.S., Marschik, R., 2005. Iron oxide copper–gold deposits; geology, space–time distribution, and possible modes of origin. Economic Geology 100th Anniversary Volume, 371–405.
Woodall, R., 1983. Success in mineral exploration: a matter of confidence. Geoscience Canada 11, 41–56.
Wyborn, L.A.I., Heinrich, C.A., Jaques, A.L., 1994. Australian Proterozoic mineral systems: essential ingredients and mappable criteria. In: Hallenstein, P.C. (Ed.), Australian Mining Looks North — the Challenges and Choices: Australian Institute of Mining and Metallurgy Publication Series, 5, pp. 109–115.
Zhao, Z.F., Zheng, Y.F., Wei, C.S., Gong, B., 2004. Temporal relationship between granitic cooling and hydrothermal uranium mineralisation at Dalongshan in China: a combined radiometric and oxygen isotopic study. Ore Geology Reviews 25, 221–236.